ANALYTICAL AND NUMERICAL SOLUTIONS TO ROTATING ORTHOTROPIC DISK PROBLEMS

A THESIS SUBMITTED TO
THE GRADUATE SCHOOL OF NATURAL AND APPLIED SCIENCES
OF
MIDDLE EAST TECHNICAL UNIVERSITY

BY

YASEMİN KAYA

IN PARTIAL FULFILLMENT OF THE REQUIREMENTS
FOR
THE DEGREE OF MASTER OF SCIENCE
IN
ENGINEERING SCIENCES

SEPTEMBER 2007

Approval of the thesis:

ANALYTICAL AND NUMERICAL SOLUTIONS TO ROTATING ORTHOTROPIC DISK PROBLEMS

Submitted by **YASEMİN KAYA** in partial fulfillment of the requirements for the degree of **Master of Science in Engineering Sciences Department, Middle East Technical University** by,

Prof. Dr. Canan Özgen _____
Dean, Graduate School of **Natural and Applied Sciences**

Prof. Dr. Turgut Tokdemir _____
Head of Department, **Engineering Sciences**

Assoc. Prof. Dr. Ahmet N. Eraslan _____
Supervisor, **Engineering Sciences Dept., METU**

Examining Committee Members:

Prof. Dr. Yusuf Orçan _____
Engineering Sciences Dept., METU

Assoc. Prof. Dr. Ahmet N. Eraslan _____
Engineering Sciences Dept., METU

Prof. Dr. Turgut Tokdemir _____
Engineering Sciences Dept., METU

Prof. Dr. Polat Saka _____
Engineering Sciences Dept., METU

Prof. Dr. Nurcan Baç _____
Chemical Engineering Dept., METU

Date: September 7, 2007

I hereby declare that all information in this document has been obtained and presented in accordance with academic rules and ethical conduct. I also declare that, as required by these rules and conduct, I have fully cited and referenced all material and results that are not original to this work.

Name, Last name : Yasemin Kaya

Signature :

ABSTRACT

ANALYTICAL AND NUMERICAL SOLUTIONS TO
ROTATING ORTHOTROPIC DISK PROBLEMS

Kaya, Yasemin
M.S., Department of Engineering Sciences
Supervisor: Assoc. Prof. Dr. Ahmet N. Eraslan

September 2007, 82 pages

Analytical and numerical models are developed to investigate the effect of orthotropy on the stress distribution in variable thickness solid and annular rotating disks. The plastic treatment is based on Hill's quadratic yield criterion, total deformation theory, and Swift's hardening law. The elastic-plastic stress distributions, residual stresses and radial displacement distributions are obtained after having analysed the cases of rotating solid disk, annular disk with rigid inclusion, annular disk subjected to either internal or external pressure. Thermal loading is also considered for the annular disk with rigid inclusion. Effects of different values of elastic and plastic orthotropy parameters are investigated. It is observed that the elastic orthotropy significantly affects the residual stresses in disks. The most remarkable effect of the plastic orthotropy is observed on the disk with rigid inclusion.

Key words: Elastoplasticity; Rotating disk; Anisotropy; Nonlinear hardening; Hill's criterion.

ÖZ

DÖNEN ORTOTROPİK DİSK PROBLEMLERİNİN ANALİTİK VE SAYISAL ÇÖZÜMLERi

Kaya, Yasemin
Yüksek Lisans, Mühendislik Bilimleri Bölümü
Tez Yöneticisi: Doç. Dr. Ahmet N. Eraslan

Eylül 2007, 82 sayfa

Değişken kalınlıklı içi dolu ve içi boş dönen disklerde ortotropinin disk içindeki gerilme dağılımına etkisini araştırmak için analitik ve sayısal modeller geliştirilmiştir. Plastik model , Hill'in kuadratik akma kriteri, toplam deformasyon teorisi ve Swift tipinde pekleşme kanununa dayanmaktadır. Elastik-plastik gerilme dağılımları, kalıntı gerilmeler ve radyal yer değiştirme dağılımları dönen içi dolu disk, rijit mile monte edilmiş içi boş dönen disk ve iç ya da dış yüzeyden basınç etkisi altındaki içi boş disk durumları için hesaplanmıştır. Rijit mile monte edilmiş içi boş disk için ısı yükü de göz önüne alınmıştır. Değişik elastik ve plastik ortotropi parametreleri için hesaplamalar yapılmıştır. Elastik ortotropi parametresinin kalıntı gerilmelerini önemli ölçüde etkilediği gözlemlenmiştir. Plastik ortotropi parametresinin ise en çok etkin olduğu durum rijit mile monte edilmiş diskte gözlemlenmiştir.

Anahtar sözcükler: Elastoplastisite; Dönen disk; Anisotropi; Lineer olmayan pekleşme; Hill kriteri.

To My Parents

ACKNOWLEDGEMENTS

I wish to express my deepest gratitude to my supervisor Assoc. Prof. Dr. Ahmet N. Eraslan for his guidance, advice, criticism, encouragements and insight throughout this study.

My special thanks are due to my family, for their great help, patience and encouragement in performing this research.

I would also like to thank to my friends, especially Özlem Aydın, for her encouragement during this research, and Ergin Taşkan, for his neverending patience, help and support.

TABLE OF CONTENTS

LIST OF FIGURES

FIGURES

CHAPTER 1

INTRODUCTION

Determination of stress distribution of disks rotating at high speeds has been given widespread attention due to a large number of applications in mechanical and structural engineering. Among these applications turbine rotors, high speed gears, flywheels, and shrink fits can be mentioned. Analysis of stresses and displacement of such structures of isotropic materials was discussed in many textbooks [1-2].

Elastic-plastic analytical or numerical solutions for isotropic rotating disks exist in literature. Güven [3-7] widely investigated rotating disk problems with various boundary conditions under different basic assumptions and obtained closed form and numerical solutions. Eraslan, Eraslan and Orçan, Eraslan and Argeşo presented closed form and numerical solutions by using different assumptions for linear and nonlinear strain hardening disks with variable thickness under different boundary conditions [8-15]. You et. al. [16-17] developed analytical and numerical solutions to determine the stresses and deformation in nonlinear strain hardening rotating disks by using Von Mises yield criterion, its associated flow rule and deformation theory of plasticity. Rees [18] derived elastic-plastic stress distributions for a disk rotating at high speeds by combining Von Mises and Tresca yield criteria and compared these criteria. Ma et. al. [19] studied plastic limit analysis of a rotating solid or annular disk in terms of a unified yield condition. Alexandrova and Alexandrov [20] investigated elastic-plastic stress distribution in a rotating annular disk. The same authors [21] also determined the displacement field and strain distribution in a rotating annular disk.

Although isotropic disks have been studied extensively, there is rare study in the literature about anisotropic disks. However, increasing the usage of anisotropic materials in the engineering applications, investigation of elastic-plastic anisotropic rotating disks has been of grate importance. Durban and Birman [22] analyzed the elastic-plastic behavior of rotating annular disk according to Hill's anisotropic flow theory. Tütüncü [23] studied the effect of anisotropy on inertio-elastic instability of rotating polar orthotropic disks. Çallıoğlu and Topçu [24] developed an analytical solution to elastic-plastic stress analysis of an orthotropic rotating disk by using Tsai-Hill theory as a yield criterion. They obtained the result that plastic yielding occurs first at the inner surface. Magnitude of circumferential stresses is found to be higher than that of the radial stress component throughout the disk. Alexandrova and Alexandrov [25] presented a semi-analytical solution to investigate the effect of anisotropy on the stress distribution in the rotating annular disk adopting Hill's quadratic yield criterion and its associated flow rule. Alexandrova and Real [26] investigated the singularities in a solution to a rotating orthotropic disk of constant thickness and density. They used Hill's quadratic orthotropic yield criterion and also considered temperature effect. Jain et. al. [27] obtained a unified formulation for studying stresses in rotating polarly orthotropic disks, shells and conical shells. They focused on the investigation of singularities circumferential modulus of elasticity is smaller than the radial modulus. The same authors [28] considered a rotating orthotropic disk of uniform thickness to show that the orthotropy parameter can be varied in such a way that it leads to equal radial and circumferential stresses.

The objective of the present work is to investigate the effect of orthotropy on stress, strain and displacement distributions in rotating disks. Pressure and thermal loading are also taken into account. For this purpose, analytical and numerical solutions are developed.

CHAPTER 2

THEORY

2.1 The Stress-Strain Diagram

To obtain the stress-strain diagram of a material, the most usual test type conducted on a specimen of the material is tensile test. The result of this test is represented by plotting the nominal stress against the conventional or engineering strains as depicted in Fig. 2.1. Nominal stress is represented by

$$\sigma_n = \frac{P}{A_0}, \tag{2.1}$$

and engineering strain by

$$\varepsilon = \frac{l - l_0}{l_0}, \tag{2.2}$$

where P is load, A_0 is original cross-sectional area, l_0 is unit original length, and l is the final length after the test.

If the load is increased, length of the specimen increases linearly up to point A, which is known as proportional limit. This portion of the stress-strain diagram is a straight line and obeys the Hooke's law. If a further increase occurs after this point, the strain no longer increases linearly but the material is still elastic. In other words, upon release of the load the specimen returns to its original length. This condition continues up to the point B, called as elastic limit or yield point. There is usually little difference between proportional limit A and elastic limit B. They are assumed the same for most materials. Point B shows

the end of elastic straining and initiation of plastic deformation. After the point B, the strain increases at a greater rate. But, the specimen will not deform further unless the load is increased. This condition is defined as work hardening or strain hardening. At point C a maximum load is reached. Beyond C the specimen neck down and fractures at D. The maximum load point C is called the tensile strength or ultimate strength.

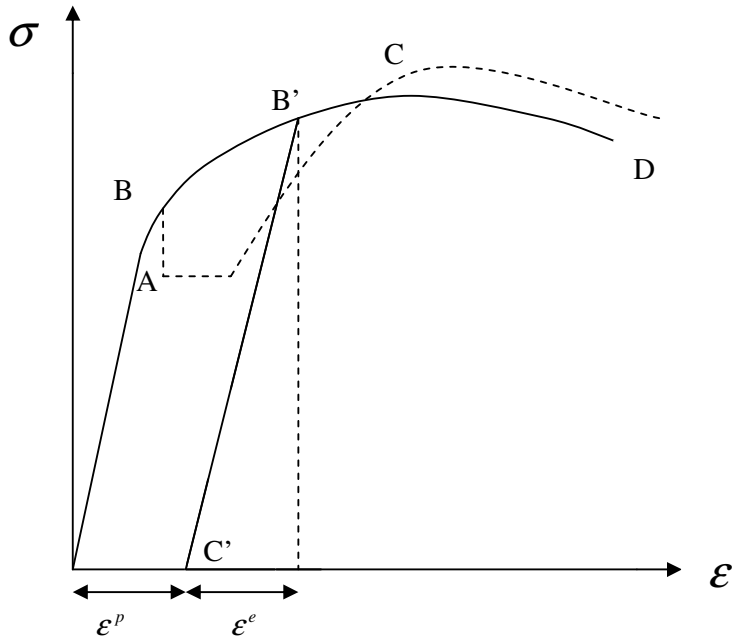

Figure 2.1 The stress-strain curve.

In the Fig. 2.1 , line B'C' shows the unloading path when the load is removed at any point between B and C. Some part of strain is recovered, which is elastic part of the strain ε^e, and other part remains permanently, which is plastic part of the strain ε^p. Therefore, total strain is presented by

$$\varepsilon = \varepsilon^e + \varepsilon^p \tag{2.3}$$

2.2 Anisotropic Yield Criterion

Annealed material may be considered as isotropic. However, if it is in any degree worked, it becomes anisotropic, i.e. its stress-strain behavior becomes direction-dependent and the texture of the material takes on a fibrous appearance. This occurs in all metal-working processes [30].

A metal in which the grains are initially oriented at random, and which is therefore isotropic, is rendered anisotropic during plastic deformation. Hill [31] presented a yield criterion assumed to be quadratic in the stress components, in the form:

$$\begin{aligned} 2f(\sigma_{ij}) &= F(\sigma_y - \sigma_z)^2 + G(\sigma_z - \sigma_x)^2 + H(\sigma_x - \sigma_y)^2 \\ &\quad + 2L\tau_{yz}^2 + 2M\tau_{zx}^2 + 2N\tau_{xy}^2 = 1 \end{aligned} \tag{2.4}$$

where F,G,H,L,M,N are parameters defining characteristics of a current state of anisotropy. The absence of linear terms in the yield function implies that there is no Bauschinger effect.

In the case of complete spherical symmetry or isotropy

$3F = 3G = 3H = L = M = N$,

and Eqn.(2.4) reduces to von Mises' criterion. The yield criterion is represented in the form of Eqn.(2.4) only when the principal axes of anisotropy are taken as the axes of reference.

For the orthotropic material, it is chosen that rectangular axes coincide with the principal axes of anisotropy. According to Hill's criterion, the effective stress σ_e is represented for the polar coordinates by

$$2(1+R)\sigma_e^M = (1+2R)\left|\sigma_r - \sigma_\theta\right|^M + \left|\sigma_r + \sigma_\theta\right|^M, \tag{2.5}$$

where the parameters R and M characterize the normal plastic anisotropy of the disk. For the rotating disk $\sigma_r - \sigma_\theta < 0$, and $\sigma_r + \sigma_\theta > 0$ [22]. If $M = 2$, Eqn.(2.5) reduces to

$$2(1+R)\sigma_e^2 = (1+2R)(\sigma_r - \sigma_\theta)^2 + (\sigma_r + \sigma_\theta)^2, \tag{2.6}$$

which is Hill's orthotropic yield function. If $R = 1$, material is said to be isotropic, and Eqn.(2.6) reduces to von Mises' criterion.

CHAPTER 3

PROBLEM DEFINITION AND SOLUTION

In this study, a rotating disk that has an inner radius a and outer radius b is considered. It is assumed that the thickness of the disk , h, changes according to the following parabolic function:

$$h(r) = h_0\left[1 - n\left(\frac{r}{b}\right)^k\right], \tag{3.1}$$

where h_0 is the thickness of the disk at $r = 0$; n and k are parameters $(n > 0, k > 0)$, which describe thickness variation. In the case that $n \to \infty$, thickness of disk becomes uniform. If $k = 1$, the disk has a linearly decreasing thickness profile; if $k < 1$, it is concave, and if $k > 1$, it is convex.

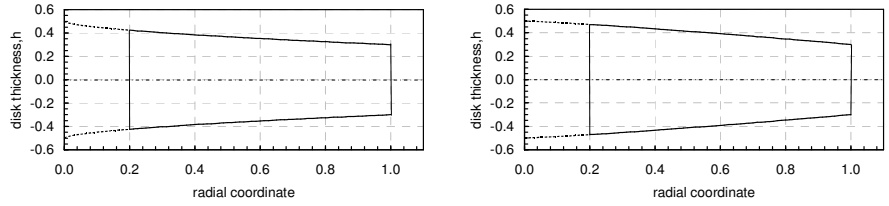

(a) (b)

Figure 3.1 Disk profiles (a) concave for $n = 0.4$ and $k = 0.6$ and (b) convex for $n = 0.4$ and $k = 1.2$.

3.1 Basic Equations

In the solution Timoshenko and Goodier notation is used. The thickness of the disk is small in comparison with its radius; therefore, stresses can be neglected throughout the disk thickness and the problem can be solved as the plane stress condition.

The equation of motion of the rotating disk with variable thickness can be written as [1]

$$\frac{d}{dr}(hr\sigma_r) - h\sigma_\theta + h\rho\omega^2 r^2 = 0, \tag{3.2}$$

where r is the radial coordinate, σ_r and σ_θ are the radial and circumferential stresses, ρ, the constant density of the disk material, ω, the angular velocity of the disk, and h is the thickness variation function of the disk as mentioned in Eqn.(3.1). σ_r, σ_θ and h are functions of the radial coordinate r.

The relations between strains and radial displacement are:

$$\varepsilon_r = \frac{du}{dr}, \text{ and } \varepsilon_\theta = \frac{u}{r}, \tag{3.3}$$

where ε_r and ε_θ are the total radial and circumferential strains, respectively. These two equations satisfy the compatibility equation:

$$\frac{d}{dr}(r\varepsilon_r) - \varepsilon_\theta = 0. \tag{3.4}$$

Elastic and plastic deformations occur in the rotating disk. The total strains consist of elastic and plastic components:

$$\varepsilon_r = \varepsilon_r^e + \varepsilon_r^p \text{ , and } \varepsilon_\theta = \varepsilon_\theta^e + \varepsilon_\theta^p, \tag{3.5}$$

For the plane stress problems, elastic deformations in the case of anisotropy can be expressed by the following stress-strain relations based on Hooke law:

$$\varepsilon_r^e = \frac{\sigma_r}{E_r} - \frac{\nu_{\theta r}}{E_\theta}\sigma_\theta + \alpha\Theta, \tag{3.6}$$

$$\varepsilon_\theta^e = \frac{\sigma_\theta}{E_\theta} - \frac{\nu_{r\theta}}{E_r}\sigma_r + \alpha\Theta, \tag{3.7}$$

where ε_r^e and ε_θ^e are the elastic radial and circumferential strains, E_r and E_θ are Young's Modulus in r and θ directions, $\nu_{r\theta}$ and $\nu_{\theta r}$, Poisson's ratios, α ,thermal expansion coefficient, $\Theta = T(r) - T_\infty$,temperature difference between the disk surface and the surrounding temperatures for the nonisothermal case.

For the plastic deformation, considering the deformation theory of plasticity, the stress-plastic strain relations are constructed on the basis of Hill's anisotropic yield function [16, 31]:

$$\varepsilon_r^p = \frac{\varepsilon_{EQ}}{\sigma_e}\left[\sigma_r - \frac{R_2}{1+R_2}\sigma_\theta\right], \tag{3.8}$$

$$\varepsilon_\theta^p = \frac{\varepsilon_{EQ}}{\sigma_e}\left[\sigma_\theta - \frac{R_2}{1+R_2}\sigma_r\right], \tag{3.9}$$

where ε_r^p and ε_θ^p are the plastic radial and circumferential strains, ε_{EQ} is the equivalent plastic strain, σ_e , the equivalent stress. According to Hill's quadratic yield criterion, σ_e is defined as

$$\sigma_e = \sqrt{\sigma_r^2 - \frac{2R_2}{1+R_2}\sigma_r\sigma_\theta + \sigma_\theta^2}, \tag{3.10}$$

and R_2 is the plastic orthotropy parameter given before as R in Eqn. (2.6). When $\sigma_e \geq 1$, the yielding starts.

Using Swift's nonlinear strain hardening law, the relation between the equivalent stress σ_e, and the equivalent plastic strain ε_{EQ} can be written as [30]

$$\sigma_e = \sigma_0 (1 + \eta \varepsilon_{EQ})^{1/m} , \tag{3.11}$$

where σ_0 is the yield stress, η, the hardening parameter, and m, the material parameter. The inverse relation is:

$$\varepsilon_{EQ} = \left[\left(\frac{\sigma_e}{\sigma_0} \right)^m - 1 \right] \frac{1}{\eta} . \tag{3.12}$$

In order to calculate the temperature distribution throughout the disk, energy equation can be written as [32]

$$\frac{d^2}{dr^2}\Theta + \left[\frac{1}{r} + \frac{h'}{h} \right] \frac{d}{dr}\Theta - \frac{H_c}{\lambda h}\Theta = 0 , \tag{3.13}$$

where $\Theta = T(r) - T_\infty$ is the temperature difference between the surface of the disk and the surrounding temperature, h' denotes the first derivative of the disk profile function h with respect to r, H_c is the heat transfer coefficient, and λ, thermal conductivity of the disk material.

Heat transfer coefficient H_c is a function of r and ω, given by

$$H_c(r, \omega) = H_0 + H_1 \omega r + H_2 \omega^2 r^2 , \tag{3.14}$$

with the parameters H_0, H_1, and H_2.

In the solution process, basic equations are written in the dimensionless forms. For this purpose, the following nondimensional and normalized variables are defined;

Radial coordinate : $\bar{r} = \frac{r}{b}$,

Disk thickness : $\bar{h} = \frac{h}{h_0}$,

Stress : $\bar{\sigma}_j = \frac{\sigma_j}{\sigma_0}$,

Displacement : $\bar{u} = \frac{uE_r}{\sigma_0 b}$,

Strain : $\bar{\varepsilon}_j = \frac{\varepsilon_j E_r}{\sigma_0}$,

Angular velocity : $\Omega = \omega b\sqrt{\rho / \sigma_0}$,

Pressure : $\bar{P} = \frac{P}{\sigma_0}$.

The equation of motion of rotating disk with variable thickness can be written as

$$\frac{d}{d\bar{r}}(\bar{h}\bar{r}\bar{\sigma}_r) - \bar{h}\bar{\sigma}_\theta + \bar{h}\Omega^2\bar{r}^2 = 0. \tag{3.15}$$

Compatibility equation:

$$\frac{d}{d\bar{r}}(\bar{r}\bar{\varepsilon}_r) - \bar{\varepsilon}_r = 0. \tag{3.16}$$

If we define the orthotropy parameter in the elastic region as

$$R_1 = \frac{E_r}{E_\theta}, \tag{3.17}$$

and Maxwell relation is written as

$$\nu_{r\theta} = R_1\nu_{\theta r}, \tag{3.18}$$

the elastic strains become:

$$\bar{\varepsilon}_r^e = \bar{\sigma}_r - \nu_{r\theta}\bar{\sigma}_\theta + \bar{\alpha}\Theta, \tag{3.19}$$

$$\bar{\varepsilon}_\theta^e = R_1\bar{\sigma}_\theta - \nu_{r\theta}\bar{\sigma}_r + \bar{\alpha}\Theta. \tag{3.20}$$

Plastic strains:

$$\bar{\varepsilon}_r^p = \frac{\bar{\varepsilon}_{EQ}}{\bar{\sigma}_Y}\left[\bar{\sigma}_r - \frac{R_2}{1+R_2}\bar{\sigma}_\theta\right], \tag{3.21}$$

$$\bar{\varepsilon}_\theta^p = \frac{\bar{\varepsilon}_{EQ}}{\bar{\sigma}_Y}\left[\bar{\sigma}_\theta - \frac{R_2}{1+R_2}\bar{\sigma}_r\right]. \tag{3.22}$$

Equivalent plastic strain:

$$\bar{\varepsilon}_{EQ} = \frac{1}{H}\left(\bar{\sigma}_e^m - 1\right), \tag{3.23}$$

where $H = \eta\sigma_0 / E_r$ is the hardening parameter.

Hill's yield criterion for orthotropic materials:

$$\bar{\sigma}_e = \sqrt{\bar{\sigma}_r^2 - \frac{2R_2}{1+R_2}\bar{\sigma}_r\bar{\sigma}_\theta + \bar{\sigma}_\theta^2}\ . \tag{3.24}$$

Total strains are summation of the elastic and plastic strains:

$$\bar{\varepsilon}_r = \bar{\sigma}_r - \nu_{r\theta}\bar{\sigma}_\theta + \bar{\alpha}\Theta + \bar{\varepsilon}_r^p, \tag{3.25}$$

$$\bar{\varepsilon}_\theta = R_1\bar{\sigma}_\theta - \nu_{r\theta}\bar{\sigma}_r + \bar{\alpha}\Theta + \bar{\varepsilon}_\theta^p. \tag{3.26}$$

Later the following stress function will be used [1]:

$$Y = \bar{h}\bar{r}\bar{\sigma}_r. \tag{3.27}$$

The radial stress, therefore, is

$$\bar{\sigma}_r = \frac{Y}{\bar{h}\bar{r}}, \tag{3.28}$$

and if it is substituted into the equation of motion, Eqn. (3.15), circumferential stress is obtained as

$$\bar{\sigma}_\theta = \bar{r}^2\Omega^2 + \frac{1}{\bar{h}}\frac{dY}{d\bar{r}}. \tag{3.29}$$

Derivatives of stresses with respect to r are:

$$\frac{d\bar{\sigma}_r}{d\bar{r}} = -\left[\frac{1}{\bar{h}\bar{r}^2} + \frac{\bar{h}'}{\bar{h}^2\bar{r}}\right]Y + \frac{1}{\bar{h}\bar{r}}\frac{dY}{d\bar{r}}\ , \tag{3.30}$$

$$\frac{d\bar{\sigma}_\theta}{d\bar{r}} = 2\bar{r}\Omega^2 - \frac{\bar{h}'}{\bar{h}^2}\frac{dY}{d\bar{r}} + \frac{1}{\bar{h}}\frac{d^2Y}{d\bar{r}^2}. \tag{3.31}$$

Derivative of the yield stress:

$$\begin{aligned}\frac{d\bar{\sigma}_e}{d\bar{r}} &= \frac{[(1+R_2)\bar{\sigma}_r - R_2\bar{\sigma}_\theta]\bar{\sigma}_r' + [\bar{\sigma}_\theta + R_2(\bar{\sigma}_\theta - \bar{\sigma}_r)]\bar{\sigma}_\theta'}{(1+R_2)\bar{\sigma}_e} \\ &= N_1\frac{d\bar{\sigma}_r}{d\bar{r}} + N_2\frac{d\bar{\sigma}_\theta}{d\bar{r}}\end{aligned}\ , \tag{3.32}$$

where

$$N_1 = \frac{(1+R_2)\bar{\sigma}_r - R_2\bar{\sigma}_\theta}{(1+R_2)\bar{\sigma}_e}, \text{ and } N_2 = \frac{\bar{\sigma}_\theta + R_2(\bar{\sigma}_\theta - \bar{\sigma}_r)}{(1+R_2)\bar{\sigma}_e}. \tag{3.33}$$

Substituting total strains, Eqn.s (3.25) and (3.26) in the compatibility, Eqn. (3.16), gives

$$\begin{aligned}&\frac{\bar{\varepsilon}_\theta^p - \bar{\varepsilon}_r^p}{\bar{r}R_1} - \frac{(1+\nu_{r\theta})\bar{\sigma}_r}{\bar{r}R_1} + \frac{(\nu_{r\theta}+R_1)\bar{\sigma}_\theta}{\bar{r}R_1} + \frac{1}{R_1}\frac{d\bar{\varepsilon}_\theta^p}{d\bar{r}} - \frac{\nu_{r\theta}}{R_1}\frac{d\bar{\sigma}_r}{d\bar{r}} \\ &\qquad + \frac{d\bar{\sigma}_\theta}{d\bar{r}} + \frac{\bar{\alpha}}{R_1}\frac{d}{d\bar{r}}\Theta = 0\end{aligned} \tag{3.34}$$

with derivative of plastic strain

$$\frac{d\bar{\varepsilon}_\theta^p}{d\bar{r}} = \left[\frac{N_1 N_4 N_5 - N_3 R_2 \bar{\sigma}_e}{H(1+R_2)\bar{\sigma}_e^2}\right]\frac{d\bar{\sigma}_r}{d\bar{r}} + \left[\frac{N_2 N_4 N_5 - N_3(1+R_2)\bar{\sigma}_e}{H(1+R_2)\bar{\sigma}_e^2}\right]\frac{d\bar{\sigma}_\theta}{d\bar{r}} \quad , \quad (3.35)$$

where

$N_3 = \bar{\sigma}_e^m - 1$,

$N_4 = N_3 - m\bar{\sigma}_e^m$,

$N_5 = R_2\bar{\sigma}_r - (1+R_2)\bar{\sigma}_\theta$.

3.2 Temperature Distribution

In the problem, nonisothermal case is calculated only for the rigid inclusion case. Temperature distribution is calculated numerically. The following dimensionless parameters are defined;

Thermal expansion coefficient : $\bar{\alpha} = \dfrac{E_r \alpha}{\sigma_0}$,

Heat transfer coefficient : $\bar{H}_c = \dfrac{H_c b}{\lambda}$,

Heat load : $\bar{q} = -\dfrac{\bar{\alpha} T_b}{\log(\bar{a})}$.

Energy equation is rearranged as follows:

$$\frac{d^2}{d\bar{r}^2}\Theta + \left[\frac{1}{\bar{r}} + \frac{\bar{h}'}{\bar{h}}\right]\frac{d}{d\bar{r}}\Theta - \frac{\bar{H}_c}{\bar{h}_0\bar{h}}\Theta = 0, \quad (3.36)$$

where $\bar{h}_0 = h_0 / b$, and the heat transfer coefficient H_c is used in the dimensionless form as

$$\bar{H}_c(\bar{r},\Omega) = \bar{H}_0 + \bar{H}_1\Omega\bar{r} + \bar{H}_2\Omega^2\bar{r}^2. \quad (3.37)$$

Boundary conditions for annular disk:

$$\Theta(a) = T_b - T_\infty \text{ , and } \quad -k\left.\frac{d\Theta}{dr}\right|_{r=b} = H_c(b,\omega)\left[T(b) - T_\infty\right], \tag{3.38}$$

where $T_b = -\bar{q}\log(\bar{a})/\bar{\alpha}$, is the temperature of the hot rigid shaft found from the heat load. If the surrounding temperature T_∞ is taken as zero, boundary conditions can be written in the following form:

$$\Theta(\bar{a}) = T_b \text{ , and } \left.\frac{d\Theta}{d\bar{r}}\right|_{\bar{r}=1} = \overline{H}_c(1,\Omega)\Theta(1). \tag{3.39}$$

This two point boundary value problem can be converted to an initial value problem, IVP, and solved numerically by shooting method as follows:

$$\frac{d^2\Theta}{d\bar{r}^2} = f\left(\bar{r}, \Theta, \frac{d\Theta}{d\bar{r}}\right), \tag{3.40}$$

and, if Θ and its derivative is defined as $\phi_1 = \Theta$ and $\phi_2 = \dfrac{d\Theta}{d\bar{r}}$, thus,

$$\frac{d\phi_1}{d\bar{r}} = \frac{d\Theta}{d\bar{r}} = \phi_2, \text{ and } \quad \frac{d\phi_2}{d\bar{r}} = \frac{d^2\Theta}{d\bar{r}^2} = f(\bar{r}, \phi_1, \phi_2), \text{ or}$$

$$\begin{aligned} \frac{d\phi_1}{d\bar{r}} &= \phi_2, \\ \frac{d\phi_2}{d\bar{r}} &= -\left[\frac{1}{\bar{r}} + \frac{\bar{h}'}{\bar{h}}\right]\phi_2 - \frac{\overline{H}_c}{\bar{h}\bar{h}_0}\phi. \end{aligned} \tag{3.41}$$

For this initial value problem, the initial conditions are that $\phi_1(\bar{a}) = T_b$, $\phi_2(\bar{a})$ is unknown. Right boundary condition is written in the same form as $\phi_2(1) = \overline{H}_c(1,\Omega)\phi_1(1)$. Since $\phi_2(\bar{a})$ is not known, it is assumed, and the estimation is improved by Newton iteration scheme. For this purpose, the IVP is solved numerically three times for k^{th} iteration cycle as follows:

I. $\phi_2(\bar{a}) = \phi_2^k(\bar{a})$ to give $F_1 = \phi_1(1) + \frac{1}{\bar{H}_c}\phi_2(1)$

II. $\phi_2(\bar{a}) = \phi_2^k(\bar{a}) + \Delta\phi$ to give $F_2 = \phi_1(1) + \frac{1}{\bar{H}_c}\phi_2(1)$ (3.42)

III. $\phi_2(\bar{a}) = \phi_2^k(\bar{a}) - \Delta\phi$ to give $F_3 = \phi_1(1) + \frac{1}{\bar{H}_c}\phi_2(1)$

where $\bar{a} = a/b$,and $\Delta\phi$ is a small increment. A better approximated value of $\phi_2(\bar{a})$ is obtained from:

$$\phi_2^{k+1}(\bar{a}) = \phi_2^k(\bar{a}) - \frac{2\Delta\phi F_1}{F_2 - F_3} \tag{3.43}$$

If $\left|\phi_2^{k+1}(\bar{a}) - \phi_2^k(\bar{a})\right| < \varepsilon_T$, iteration will stop and the IVP is solved numerically by using Runge-Kutta Fehlberg predictor corrector method for the last estimation of $\phi_2(\bar{a})$ value. In addition, ε_T is the error tolerance, which is taken as 10^{-9}.

3.3 Elastic Analytical Solution

Elastic part of the Eqn.(3.35) is:

$$-\frac{(1+\nu_{r\theta})\bar{\sigma}_r}{\bar{r}R_1} + \frac{(\nu_{r\theta}+R_1)\bar{\sigma}_\theta}{\bar{r}R_1} - \frac{\nu_{r\theta}}{R_1}\frac{d\bar{\sigma}_r}{d\bar{r}} + \frac{d\bar{\sigma}_\theta}{d\bar{r}} + \frac{\bar{\alpha}}{R_1}\frac{d\Theta}{d\bar{r}} = 0\,. \tag{3.44}$$

Using the stresses in the form of

$$\bar{\sigma}_r = \frac{Y}{\bar{h}\bar{r}}, \text{ and } \bar{\sigma}_\theta = \bar{r}^2\Omega^2 + \frac{1}{\bar{h}}\frac{dY}{d\bar{r}}, \tag{3.45}$$

and parabolic disk profile:

$$\bar{h}(\bar{r}) = 1 - n\bar{r}^k\,, \tag{3.46}$$

elastic equation Eqn.(3.44) becomes:

$$\bar{r}^2(1-n\bar{r}^k)\frac{d^2Y}{d\bar{r}^2}+\bar{r}[1-(1-k)n\bar{r}^k]\frac{dY}{d\bar{r}}-\left[\frac{1-(1-k\nu_{r\theta})n\bar{r}^k}{R_1}\right]Y=$$

$$-\frac{(1-n\bar{r}^k)^2(\nu_{r\theta}+3R_1)\Omega^2\bar{r}^3}{R_1}-\frac{(1-n\bar{r}^k)^2\bar{r}^2\bar{\alpha}}{R_1}\frac{d\Theta}{d\bar{r}} \quad . \qquad (3.47)$$

General solution of this equation is:

$$Y(\bar{r})=C_1Y_1(\bar{r})+C_2Y_2(\bar{r})+P(\bar{r}), \qquad (3.48)$$

where

$$\begin{aligned} &Y_1(\bar{r})=\bar{r}^{-M}F(\alpha,\beta,\delta;n\bar{r}^k),\\ &Y_1(\bar{r})=\bar{r}^{M}F(\alpha-\delta+1,\beta-\delta+1,2-\delta;n\bar{r}^k),, \qquad (3.49)\\ &P(\bar{r})=U_1Y_1+U_2Y_2, \end{aligned}$$

$$M=\frac{1}{\sqrt{R_1}}. \qquad (3.50)$$

$F(\alpha,\beta,\delta;n\bar{r}^k)$ is the hypergeometric function with the following arguments:

$$\begin{aligned} F(\alpha,\beta,\delta;n\bar{r}^k)=1+\frac{\alpha\beta}{\delta 1!}z+\frac{\alpha(\alpha+1)\beta(\beta+1)}{\delta(\delta+1)2!}z^2\\ +\frac{\alpha(\alpha+1)(\alpha+2)\beta(\beta+1)(\beta+2)}{\delta(\delta+1)(\delta+2)3!}z^3+..., \end{aligned} \qquad (3.51)$$

$$\begin{aligned} &\alpha=-\frac{1}{2}-\frac{M}{k}-\frac{M\sqrt{4(1-k\nu_{r\theta})+k^2R_1}}{2k}\\ &\beta=-\frac{1}{2}-\frac{M}{k}+\frac{M\sqrt{4(1-k\nu_{r\theta})+k^2R_1}}{2k} \qquad (3.52)\\ &\delta=1-\frac{2M}{k} \end{aligned}$$

$$U_1(\bar{r}) = \int_{\bar{a}}^{\bar{r}} G_1(\lambda) d\lambda \;\; ; \;\; U_2(\bar{r}) = \int_{\bar{a}}^{\bar{r}} G_2(\lambda) d\lambda \tag{3.53}$$

$$G_1(\bar{r}) = -\frac{Y_2(\bar{r}) f(\bar{r})}{W_{r0}(\bar{r})} \text{ , and } G_2(\bar{r}) = \frac{Y_1(\bar{r}) f(\bar{r})}{W_{r0}(\bar{r})} \tag{3.54}$$

$$f(\bar{r}) = -\frac{(1 - n\bar{r}^k)(\nu_{r\theta} + 3R_1)\Omega^2 \bar{r}}{R_1} - \frac{\bar{\alpha}}{R_1} \frac{d\Theta}{d\bar{r}} \tag{3.55}$$

$$W_{r0}(\bar{r}) = Y_1(\bar{r}) Y_2^{'}(\bar{r}) - Y_2(\bar{r}) Y_1^{'}(\bar{r}) \tag{3.56}$$

U_1 and U_2 are evaluated by expanding the integrals in series at Gaussian points:

$$U_1(\bar{r}) = \frac{\bar{r} - \bar{a}}{2} \sum_{i=1}^{N} \phi_i \times G_1\left(\frac{(\bar{r} - \bar{a}) X_i + \bar{r} + \bar{a}}{2} \right) \tag{3.57}$$

$$U_2(\bar{r}) = \frac{\bar{r} - \bar{a}}{2} \sum_{i=1}^{N} \phi_i \times G_2\left(\frac{(\bar{r} - \bar{a}) X_i + \bar{r} + \bar{a}}{2} \right) \tag{3.58}$$

Note that $U_1(\bar{a}) = U_2(\bar{a}) = 0$, and $P(\bar{a}) = 0$.

3.3.1 Boundary Conditions

In this problem, five different cases of the disk are taken into account, rotating solid disk, rotating annular disk, rotating annular disk with rigid inclusion, annular disk subjected to internal pressure and annular disk subjected to external pressure.

We note that from Eqn. (3.20), the radial displacement takes the form:

$$\bar{u}(\bar{r}) = R_1\Omega^2\bar{r}^3 - \frac{\nu_{r\theta}}{\bar{h}}Y + \frac{\bar{r}R_1}{\bar{h}}\frac{dY}{d\bar{r}} + \bar{r}\bar{\alpha}T \tag{3.59}$$

3.3.2 Rotating Solid Disk

Stresses are finite at $\bar{r} = 0$. From Eqn. (3.27) $Y(0) = 0$, and from Eqn. (3.49), $C_1 = 0$. From $\bar{\sigma}_r(1) = 0$, $Y(1) = 0$, and

$$C_2 = -\frac{P(1)}{Y_2(1)} \tag{3.60}$$

In this case, as $\bar{h}(0) = 1$, we can show that:

$$\bar{\sigma}_r(0) = \bar{\sigma}_\theta(0) = \frac{dY}{d\bar{r}} \text{ , and } \bar{u}(0) = 0 \tag{3.61}$$

3.3.3 Rotating Annular Disk

Boundary conditions are $\bar{\sigma}_r(\bar{a}) = 0$, and $\bar{\sigma}_r(1) = 0$. Integration constants are found to be:

$$C_1 = -\frac{P(1)Y_2(\bar{a})}{Y_1(\bar{a})Y_2(1) - Y_1(1)Y_2(\bar{a})} \tag{3.62}$$

$$C_2 = -\frac{P(1)Y_1(\bar{a})}{Y_1(1)Y_2(\bar{a}) - Y_1(\bar{a})Y_2(1)} \tag{3.63}$$

3.3.4 Rotating Annular Disk with Rigid Inclusion

Boundary conditions are $\bar{u}(\bar{a}) = 0$ and $\bar{\sigma}_r(1) = 0$. The result is:

$$C_1 = \frac{\bar{a}\bar{h}(\bar{a})Y_2(1)[\bar{a}^2R_1\Omega^2 + \bar{\alpha}T(\bar{a})] + P(1)[\nu_{r\theta}Y_2(\bar{a}) - \bar{a}R_1Y_2'(\bar{a})]}{Y_1(1)[\bar{a}R_1Y_2'(\bar{a}) - \nu_{r\theta}Y_2(\bar{a})] + Y_2(1)[\nu_{r\theta}Y_1(\bar{a}) - \bar{a}R_1Y_1'(\bar{a})]} \tag{3.64}$$

$$C_2 = \frac{P(1)[\bar{a}R_1 Y_1^{'}(\bar{a}) - \nu_{r\theta} Y_1(\bar{a})] - \bar{a}\bar{h}(\bar{a})Y_1(1)[\bar{a}^2 R_1 \Omega^2 + \bar{\alpha}T(\bar{a})]}{Y_1(1)[\bar{a}R_1 Y_2^{'}(\bar{a}) - \nu_{r\theta} Y_2(\bar{a})] + Y_2(1)[\nu_{r\theta} Y_1(\bar{a}) - \bar{a}R_1 Y_1^{'}(\bar{a})]} \tag{3.65}$$

3.3.5 Annular Disk Subjected to Internal Pressure

Boundary conditions are $\bar{\sigma}_r(\bar{a}) = -\bar{P}_{in}$ and $\bar{\sigma}_r(1) = 0$. The result is

$$C_1 = -\frac{\bar{a}P_{in}\bar{h}(\bar{a})Y_2(1) - \bar{P}(1)Y_2(\bar{a})}{Y_1(\bar{a})Y_2(1) - Y_1(1)Y_2(\bar{a})}, \tag{3.66}$$

$$C_2 = \frac{\bar{a}P_{in}\bar{h}(\bar{a})Y_1(1) - \bar{P}(1)Y_1(\bar{a})}{Y_1(\bar{a})Y_2(1) - Y_1(1)Y_2(\bar{a})}, \tag{3.67}$$

where $\bar{P}_{in}$ is the internal pressure.

3.3.6 Annular Disk Subjected to External Pressure

Boundary conditions are $\bar{\sigma}_r(\bar{a}) = 0$ and $\bar{\sigma}_r(1) = -\bar{P}_{ex}$. The result is

$$C_1 = \frac{Y_2(\bar{a})[P_{ex}\bar{h}(1) + \bar{P}(1)]}{Y_1(\bar{a})Y_2(1) - Y_1(1)Y_2(\bar{a})}, \tag{3.68}$$

$$C_2 = -\frac{Y_1(\bar{a})[P_{ex}\bar{h}(1) + \bar{P}(1)]}{Y_1(\bar{a})Y_2(1) - Y_1(1)Y_2(\bar{a})}, \tag{3.69}$$

where $\bar{P}_{ex}$ is the internal pressure.

3.4 Elastic-Plastic Numerical Solution

Since the first derivative of circumferential stress, $d\bar{\sigma}_\theta / d\bar{r}$, includes the second derivative of the stress function, $d^2Y / d\bar{r}^2$, elastic equation Eqn.(3.44) should be rearranged in terms of stress function as follows:

$$\underbrace{-\frac{(1+\nu_{r\theta})\bar{\sigma}_r}{\bar{r}R_1}+\frac{(\nu_{r\theta}+R_1)\bar{\sigma}_\theta}{\bar{r}R_1}-\frac{\nu_{r\theta}}{R_1}\frac{d\bar{\sigma}_r}{d\bar{r}}+\frac{\bar{\alpha}}{R_1}\frac{d\Theta}{d\bar{r}}}_{K}+\frac{d\bar{\sigma}_\theta}{d\bar{r}}=0,$$

$$K+\frac{d\bar{\sigma}_\theta}{d\bar{r}}=0. \tag{3.70}$$

Substituting derivative of circumferential stress into the above equation, it can be written in terms of stress function:

$$K+2\bar{r}\Omega^2-\frac{\bar{h}'}{\bar{h}}\frac{dY}{d\bar{r}}+\frac{1}{\bar{h}}\frac{d^2Y}{d\bar{r}^2}=0. \tag{3.71}$$

If Eqn.(3.71) is rearranged, a second order ordinary differential equation is obtained:

$$\frac{d^2Y}{d\bar{r}^2}=-\bar{h}\left[K+2\bar{r}\Omega^2-\frac{\bar{h}'}{\bar{h}}\frac{dY}{d\bar{r}}\right]. \tag{3.72}$$

In the plastic case, derivative of circumferential plastic strain also includes the second derivative of stress function indicated below:

$$\frac{d\bar{\varepsilon}_\theta^p}{d\bar{r}}=\underbrace{\left[\frac{N_1N_4N_5-N_3R_2\bar{\sigma}_Y}{H(1+R_2)\bar{\sigma}_Y^2}\right]\frac{d\bar{\sigma}_r}{d\bar{r}}}_{A}+\underbrace{\left[\frac{N_2N_4N_5-N_3(1+R_2)\bar{\sigma}_Y}{H(1+R_2)\bar{\sigma}_Y^2}\right]}_{B}\frac{d\bar{\sigma}_\theta}{d\bar{r}},$$

$$\frac{d\bar{\varepsilon}_\theta^p}{d\bar{r}}=A+B\frac{d\bar{\sigma}_\theta}{d\bar{r}}. \tag{3.73}$$

If Eqn. (3.73) is substituted into the Eqn.(3.34), we obtain:

$$\underbrace{\frac{\bar{\varepsilon}_\theta^{\,p}-\bar{\varepsilon}_r^{\,p}}{\bar{r}R_1}-\frac{(1+\nu_{r\theta})\bar{\sigma}_r}{\bar{r}R_1}+\frac{(\nu_{r\theta}+R_1)\bar{\sigma}_\theta}{\bar{r}R_1}-\frac{\nu_{r\theta}}{R_1}\frac{d\bar{\sigma}_r}{d\bar{r}}+\frac{\bar{\alpha}}{R_1}\frac{d\Theta}{d\bar{r}}}_{L}+\frac{1}{R_1}\frac{d\bar{\varepsilon}_\theta^{\,p}}{d\bar{r}}+\frac{d\bar{\sigma}_\theta}{d\bar{r}}=0$$

$$L+\frac{1}{R_1}\left[A+B\frac{d\bar{\sigma}_\theta}{d\bar{r}}\right]+\frac{d\bar{\sigma}_\theta}{d\bar{r}}=0$$

$$L+\frac{A}{R_1}+\underbrace{\left[\frac{B}{R_1}+1\right]}_{C}\frac{d\bar{\sigma}_\theta}{d\bar{r}}=0 \tag{3.74}$$

Inserting derivative of circumferential stress, $d\bar{\sigma}_\theta / d\bar{r}$, in terms of stress functions into Eqn. (3.74), a second order ordinary differential equation is obtained.

$$L+\frac{A}{R_1}+C\left[2\bar{r}\Omega^2-\frac{\bar{h}'}{\bar{h}}\frac{dY}{d\bar{r}}\right]+\frac{C}{\bar{h}}\frac{d^2Y}{d\bar{r}^2}=0 \tag{3.75}$$

$$\frac{d^2Y}{d\bar{r}^2}=-\frac{\bar{h}}{C}\left[L+\frac{A}{R_1}+C\left[2\bar{r}\Omega^2-\frac{\bar{h}'}{\bar{h}}\frac{dY}{d\bar{r}}\right]\right] \tag{3.76}$$

For both elastic and plastic cases, right hand sides of Eqn.(3.72) and Eqn.(3.76) are functions of Y and $dY/d\bar{r}$.

$$\frac{d^2Y}{d\bar{r}^2}=f\left(\bar{r},Y,\frac{dY}{d\bar{r}}\right) \tag{3.77}$$

If we define stress function and its derivative as $\phi_1 = Y$,and $\phi_2 = dY/d\bar{r}$,this two point boundary problem can be converted into an initial value problem and solved numerically for the five cases by using Runge-Kutta Fehlberg predictor corrector method.

$$\frac{d\phi_1}{d\bar{r}}=\frac{dY}{d\bar{r}}=\phi_2 \tag{3.78}$$

$$\frac{d\phi_2}{d\bar{r}} = \frac{d^2Y}{d\bar{r}^2} = f\left(\bar{r}, Y, \frac{dY}{d\bar{r}}\right) \tag{3.79}$$

3.4.1 Rotating Solid and Annular Disk

Recall that $\bar{\sigma}_r(\bar{a}) = 0$, and $\bar{\sigma}_r(1) = 0$, thus $Y(\bar{a}) = 0$ and $Y(1) = 0$ and the conditions are rewritten as

$$\begin{aligned} &\phi_1(\bar{a}) = 0, \\ &\phi_2(\bar{a}) \rightarrow \textit{not known}, \end{aligned} \tag{3.80}$$

and

$$\phi_1(1) = 0. \tag{3.81}$$

Since $\phi_2(\bar{a})$ is not known, it is assumed and the estimation is improved by Newton iteration scheme. For this purpose, the IVP is solved numerically three times for the k[th] iteration cycle as follows:

$$\begin{aligned} &\text{I.} \quad \phi_2(\bar{a}) = \phi_2^k(\bar{a}) \qquad \text{to give } F_1 = \phi_1(1) \\ &\text{II.} \quad \phi_2(\bar{a}) = \phi_2^k(\bar{a}) + \Delta\phi \text{ to give } F_2 = \phi_1(1) \\ &\text{III.} \quad \phi_2(\bar{a}) = \phi_2^k(\bar{a}) - \Delta\phi \text{ to give } F_3 = \phi_1(1) \end{aligned} \tag{3.82}$$

A better approximated value of $\phi_2(r_0)$ is obtained from

$$\phi_2^{k+1}(\bar{a}) = \phi_2^k(\bar{a}) - \frac{2\Delta\phi F_1}{F_2 - F_3} \tag{3.83}$$

If $\left|\phi_2^{k+1}(\bar{a}) - \phi_2^k(\bar{a})\right| < \varepsilon_T$, iteration will stop and IVP is solved for the last estimation of $\phi_2(\bar{a})$.

3.4.2 Rotating Annular Disk with Rigid Inclusion

We know that boundary conditions are $\overline{u}(\overline{a}) = 0$ and $\overline{\sigma}_r(1) = 0$. Thus

$$\begin{aligned} &\phi_1(\overline{a}) \rightarrow \textit{not known}, \\ &\phi_2(\overline{a}) \rightarrow \textit{not known}, \end{aligned} \tag{3.84}$$

and

$$\phi_1(1) = 0\,. \tag{3.85}$$

In the above system, both $\phi_1(\overline{a})$ and $\phi_2(\overline{a})$ are not known and not obtained directly from the left boundary conditions. Firstly, $\phi_1(\overline{a})$ is assumed. Then, $\phi_2(\overline{a})$ is obtained by using assumed $\phi_1(\overline{a})$. For this purpose, radial and circumferential stresses are expressed in terms of stress function.

$$\overline{\sigma}_r(\overline{a}) = \frac{\phi_1(\overline{a})}{\overline{h}(\overline{a})\overline{a}}, \tag{3.86}$$

$$\overline{\sigma}_\theta(\overline{a}) = \overline{a}^2\Omega^2 + \frac{1}{\overline{h}(\overline{a})}\phi_2(\overline{a})\ . \tag{3.87}$$

Eqn. (3.86) and Eqn. (3.87) are substituted into left boundary condition, $\overline{u}(\overline{a}) = 0$, in order to obtain $\phi_2(\overline{a})$. We know that

$$\overline{\varepsilon}_\theta(\overline{a}) = R_1\overline{\sigma}_\theta - \nu_{r\theta}\overline{\sigma}_r + \overline{\alpha}\Theta + \frac{\overline{\varepsilon}_{EQ}}{\overline{\sigma}_e}\left[\overline{\sigma}_r - \frac{R_2}{1+R_2}\overline{\sigma}_\theta\right], \tag{3.88}$$

and

$$\overline{u}(\overline{a}) = \overline{\varepsilon}_\theta(\overline{a})\overline{a} \tag{3.89}$$

Since $\overline{u}(\overline{a}) = 0$, $\overline{\varepsilon}_\theta(\overline{a}) = 0$. Hence, Eqn.(3.88) is set to zero.

$$R_1\left(\bar{a}^2\Omega^2+\frac{1}{\bar{h}(\bar{a})}\phi_2(\bar{a})\right)-\nu_{r\theta}\left(\frac{\phi_1(\bar{a})}{\bar{h}(\bar{a})\bar{a}}\right)+\bar{\alpha}\Theta$$
$$+\frac{\bar{\varepsilon}_{EQ}}{\bar{\sigma}_e}\left[\left(\frac{\phi_1(\bar{a})}{\bar{h}(\bar{a})\bar{a}}\right)-\frac{R_2}{1+R_2}\left(\bar{a}^2\Omega^2+\frac{1}{\bar{h}(\bar{a})}\phi_2(\bar{a})\right)\right]=0 \tag{3.90}$$

Because the effective stress and the equivalent stress include the $\phi_i(\bar{a})$ as the following ways

$$\bar{\sigma}_e=\sqrt{\left(\frac{\phi_1}{\bar{h}\bar{a}}\right)^2-\frac{2R_2}{1+R_2}\left(\frac{\phi_1}{\bar{h}\bar{a}}\right)\left(\bar{a}^2\Omega^2+\frac{1}{\bar{h}}\phi_2\right)+\left(\bar{a}^2\Omega^2+\frac{1}{\bar{h}}\phi_2\right)^2} \tag{3.91}$$

$$\bar{\varepsilon}_{EQ}=\frac{1}{H}\left(\left(\sqrt{\left(\frac{\phi_1}{\bar{h}\bar{a}}\right)^2-\frac{2R_2}{1+R_2}\left(\frac{\phi_1}{\bar{h}\bar{a}}\right)\left(\bar{a}^2\Omega^2+\frac{1}{\bar{h}}\phi_2\right)+\left(\bar{a}^2\Omega^2+\frac{1}{\bar{h}}\phi_2\right)^2}\right)^m-1\right), \tag{3.92}$$

Eqn.(3.90) is rearranged and solved by iteration to obtain $\phi_2(\bar{a})$.

$$\phi_2(\bar{a})=\frac{\nu_{r\theta}}{\bar{a}R_1}\phi_1(\bar{a})-\frac{\bar{\alpha}\Theta\bar{h}(\bar{a})}{R_1}-\bar{a}^2\Omega^2\bar{h}(\bar{a})$$
$$+\frac{\bar{\varepsilon}_{EQ}}{R_1\bar{\sigma}_e}\left[\frac{\phi_1(\bar{a})}{\bar{a}}-\frac{R_2}{1+R_2}\left(\bar{a}^2\Omega^2+\phi_2(\bar{a})\right)\right] \tag{3.93}$$

Then, $\phi_1(\bar{a})$ value is corrected by Newton iteration scheme.

I. $\phi_1(\bar{a})=\phi_1^k(\bar{a})$ to give $F_1=\phi_1(1)$

II. $\phi_1(\bar{a})=\phi_1^k(\bar{a})+\Delta\phi$ to give $F_2=\phi_1(1)$ (3.94)

III. $\phi_1(\bar{a})=\phi_1^k(\bar{a})-\Delta\phi$ to give $F_3=\phi_1(1)$

After the assumptions and verifications the IVP is solved.

3.4.3 Annular Disk Subjected to Internal Pressure

Since $\bar{\sigma}_r(\bar{a}) = -\bar{P}_{in}$ and $\bar{\sigma}_r(1) = 0$, we can write $Y(\bar{a}) = \bar{\sigma}_r(\bar{a})\bar{h}(\bar{a})\bar{a}$ or $Y(\bar{a}) = -\bar{P}_{in}\bar{h}(\bar{a})\bar{a}$ and $Y(1) = 0$. Thus

$$\begin{aligned} &\phi_1(\bar{a}) = -\bar{P}_{in}\bar{h}(\bar{a})\bar{a}, \\ &\phi_2(\bar{a}) \rightarrow \textit{not known}, \end{aligned} \tag{3.95}$$

and

$$\phi_1(1) = 0. \tag{3.96}$$

Afterwards solution procedure is the same as the rotating annular disk.

3.4.4 Annular Disk Subjected to External Pressure

As it mentioned before, $\bar{\sigma}_r(\bar{a}) = 0$ and $\bar{\sigma}_r(1) = -\bar{P}_{ex}$. Therefore, $Y(\bar{a}) = 0$ and $Y(1) = \bar{\sigma}_r(1)\bar{h}(1)1$ or $Y(1) = -\bar{P}_{ex}h(1)$. Hence,

$$\begin{aligned} &\phi_1(\bar{a}) = 0 \\ &\phi_2(\bar{a}) \rightarrow \textit{not known} \\ &\phi_1(1) = -\bar{h}(1)\bar{P}_{ex} \end{aligned} \tag{3.97}$$

$\phi_2(\bar{a})$ is corrected by Newton iteration scheme as follows:

$$\begin{aligned} &\text{I.} \quad \phi_2(\bar{a}) = \phi_2^k(\bar{a}) \qquad \text{to give } F_1 = \phi_1(1) + \bar{h}(1)\bar{P}_{ex} \\ &\text{II.} \quad \phi_2(\bar{a}) = \phi_2^k(\bar{a}) + \Delta\phi \text{ to give } F_2 = \phi_1(1) + \bar{h}(1)\bar{P}_{ex} \\ &\text{III.} \quad \phi_2(\bar{a}) = \phi_2^k(\bar{a}) - \Delta\phi \text{ to give } F_3 = \phi_1(1) + \bar{h}(1)\bar{P}_{ex} \end{aligned} \tag{3.98}$$

and then the IVP is solved.

CHAPTER 4

RESULTS AND DISCUSSION

In this study, effects of elastic and plastic orthotropy parameters, R_1 and R_2, on disks having different boundary conditions and loads have been investigated. Whereas the plastic part of the problem is solved numerically, the analytical solution of the elastic part exists. The problem is solved for different orthotropy parameters in order to observe their effects on stress, strain, displacement, and residual stress distributions.

4.1 Elastic Analytical Solution

Results of elastic analytical solutions are presented in Figures (4.1)-(4.14). As it can be seen from the figures, the effects of R_1 have been studied.

Figures (4.1)-(4.3) show the stress and displacement distributions of rotating annular disk under the load $\Omega = 1.13845$, which is the elastic-plastic limit angular velocity on the inner surface of the disk for $R_1 = 1.4$ and $R_2 = 0.8$. It is seen that radial stress and displacement increases with the increasing value of R_1. Whereas the circumferential stress is increasing near the inner surface of disk, it decreases after a point up to the outer surface of the disk with the increasing value of R_1. Dotted lines in the figures show the isotropic case ($R_1 = 1.0$ and $R_2 = 1.0$).

Figures (4.4)-(4.6) show the effect of R_1 for the case of annular disk with rigid inclusion for the angular velocity $\Omega = 1.38381$. As seen in Fig. (4.4) , radial stresses are highly effected by variation of the R_1 in the inner surface.

Effects of R_1 on stress and displacements for the disk subjected to internal and external pressures are depicted in Figures (4.7)-(4.12). For both cases radial stresses are slightly affected by the variation of R_1. As seen in Fig. (4.8) circumferential stress decreases for the increasing values of R_1 in the inner surface of disk, while it increases near the outer surface. For the external pressure case, circumferential stress is compressive and it increases with the increasing R_1 near the inner surface and vice versa near the outer surface.

Fig. (4.13) and Fig. (4.14) show the nonisothermal case for stationary and rotating annular disks with rigid inclusion. In both cases circumferential stresses are compressive near the inner surface and tensile near the outer surface.

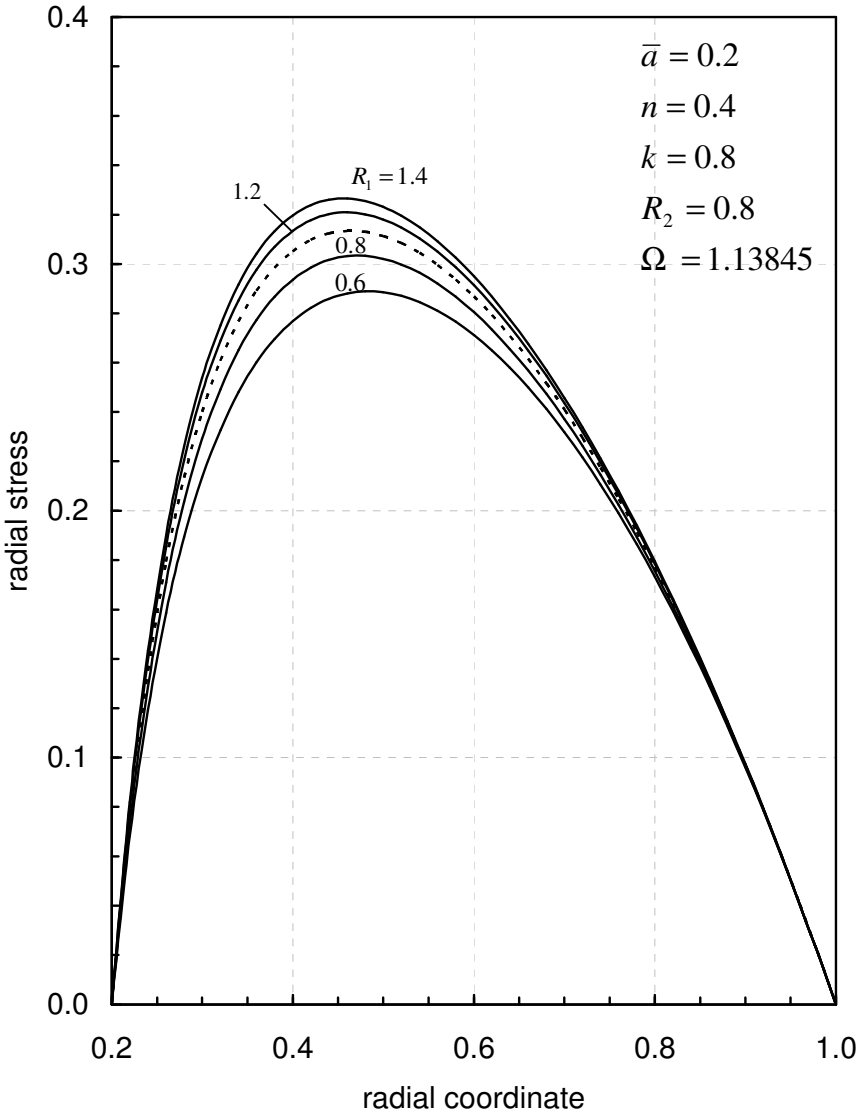

Figure 4.1 Effect of elastic orthotropy parameter R_1 on radial stress distribution for rotating annular disk.

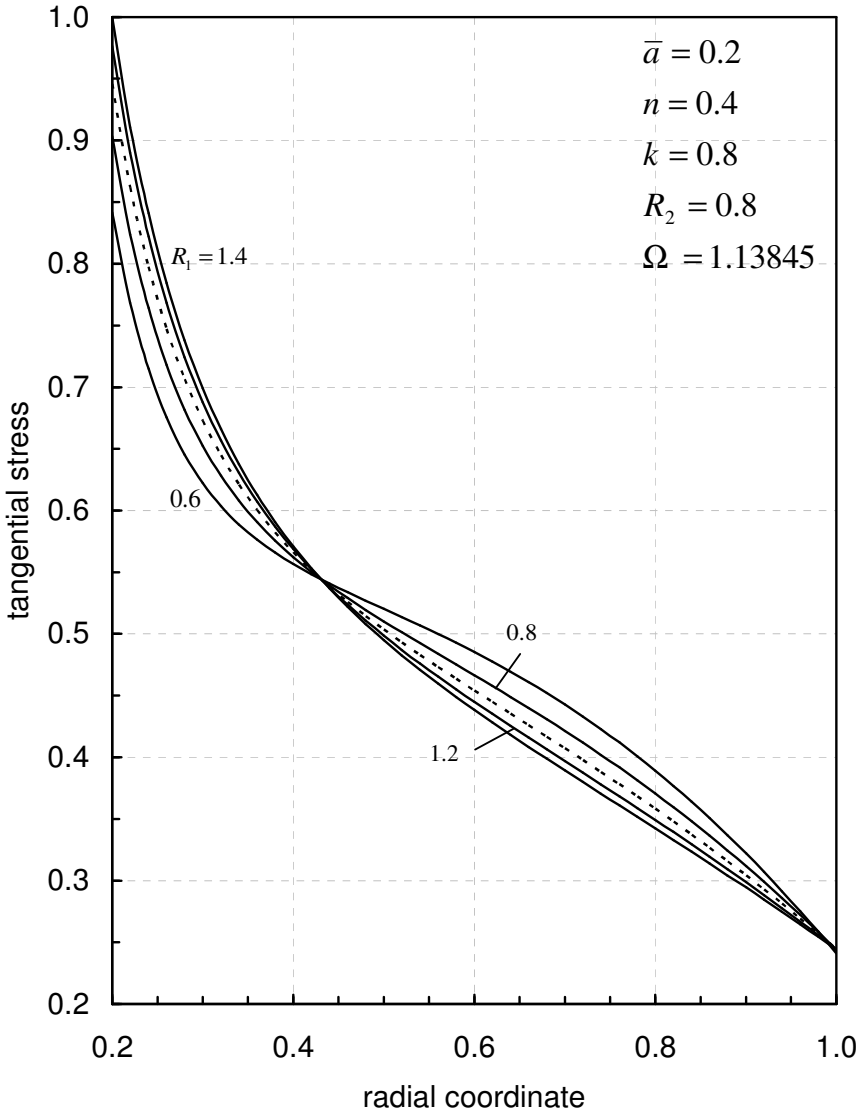

Figure 4.2 Effect of elastic orthotropy parameter R_1 on circumferential stress distribution for rotating annular disk.

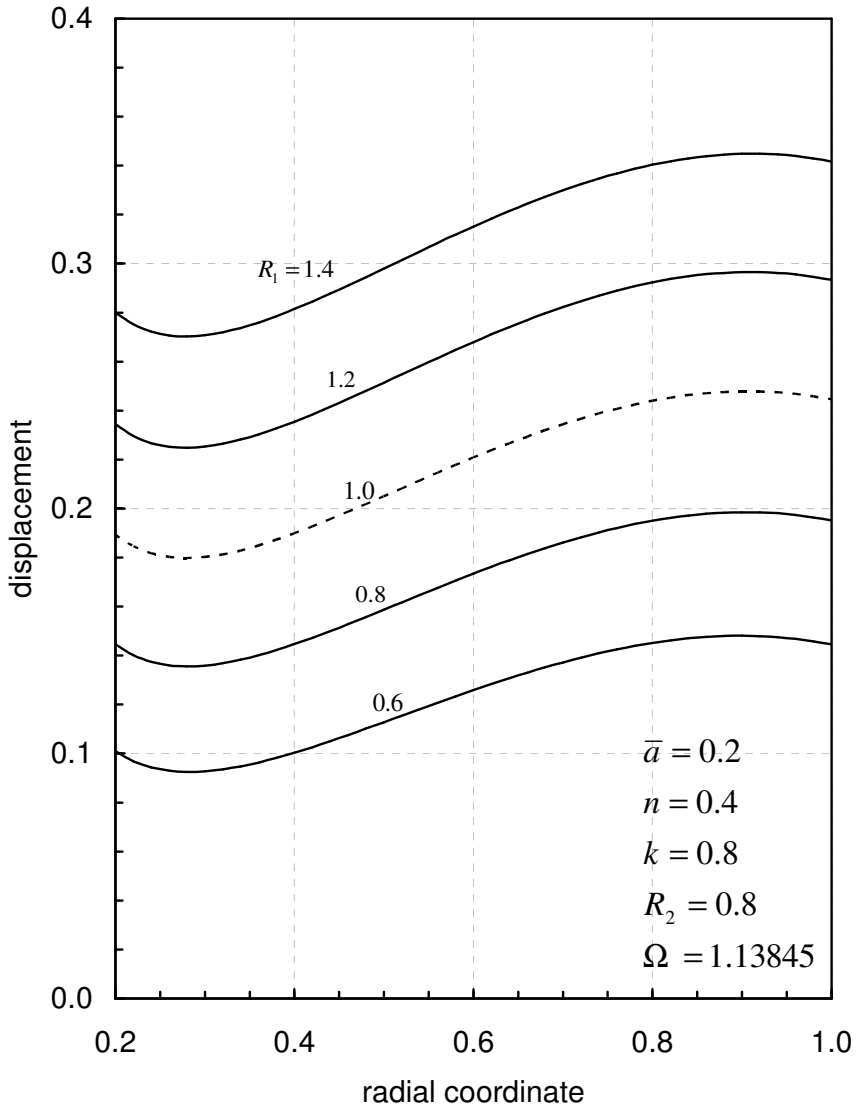

Figure 4.3 Effect of elastic orthotropy parameter R_1 on displacement for rotating annular disk.

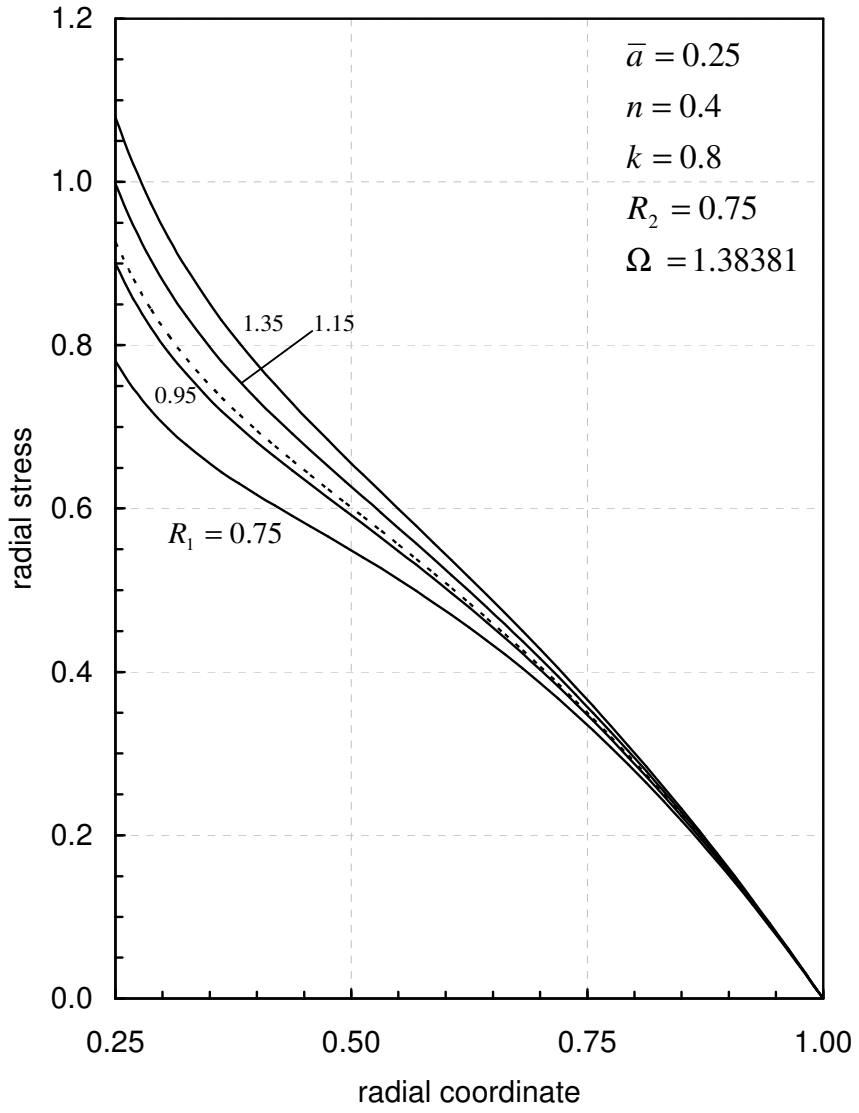

Figure 4.4 Effect of elastic orthotropy parameter R_1 on radial stress distribution for rotating annular disk with rigid inclusion.

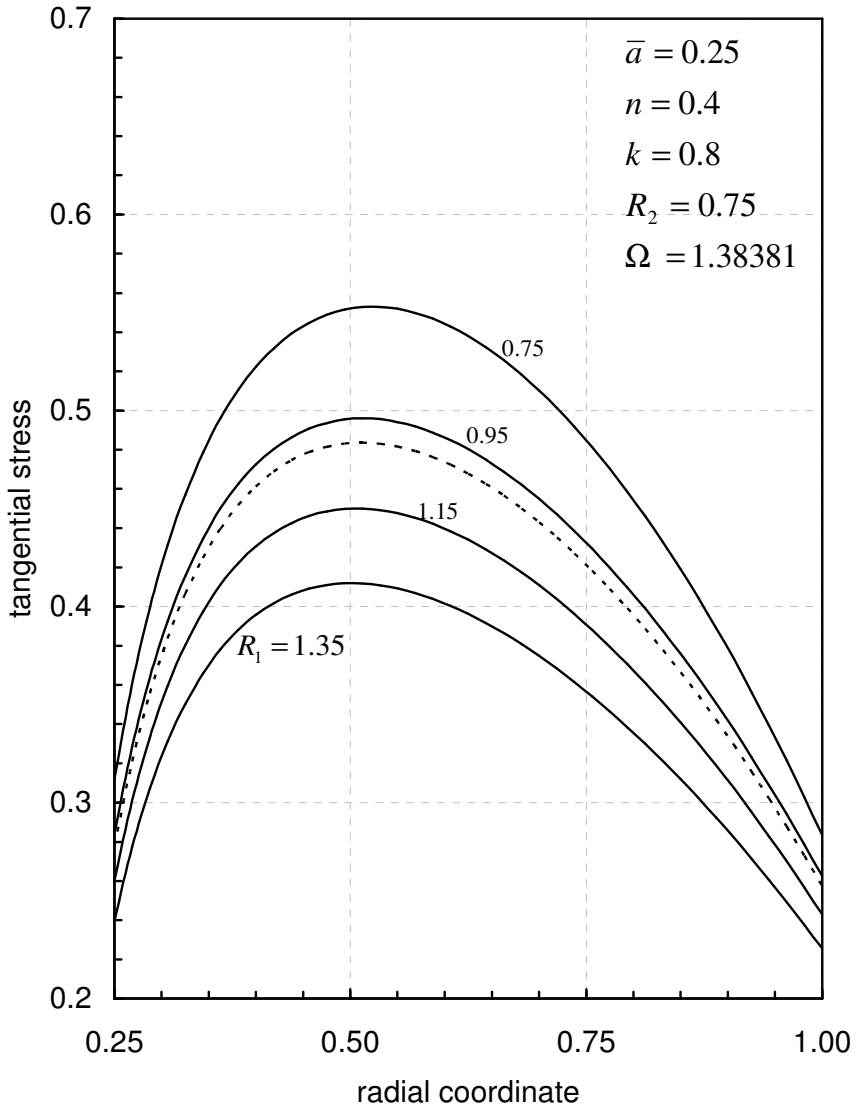

Figure 4.5 Effect of elastic orthotropy parameter R_1 on circumferential stress distribution for rotating annular disk with rigid inclusion.

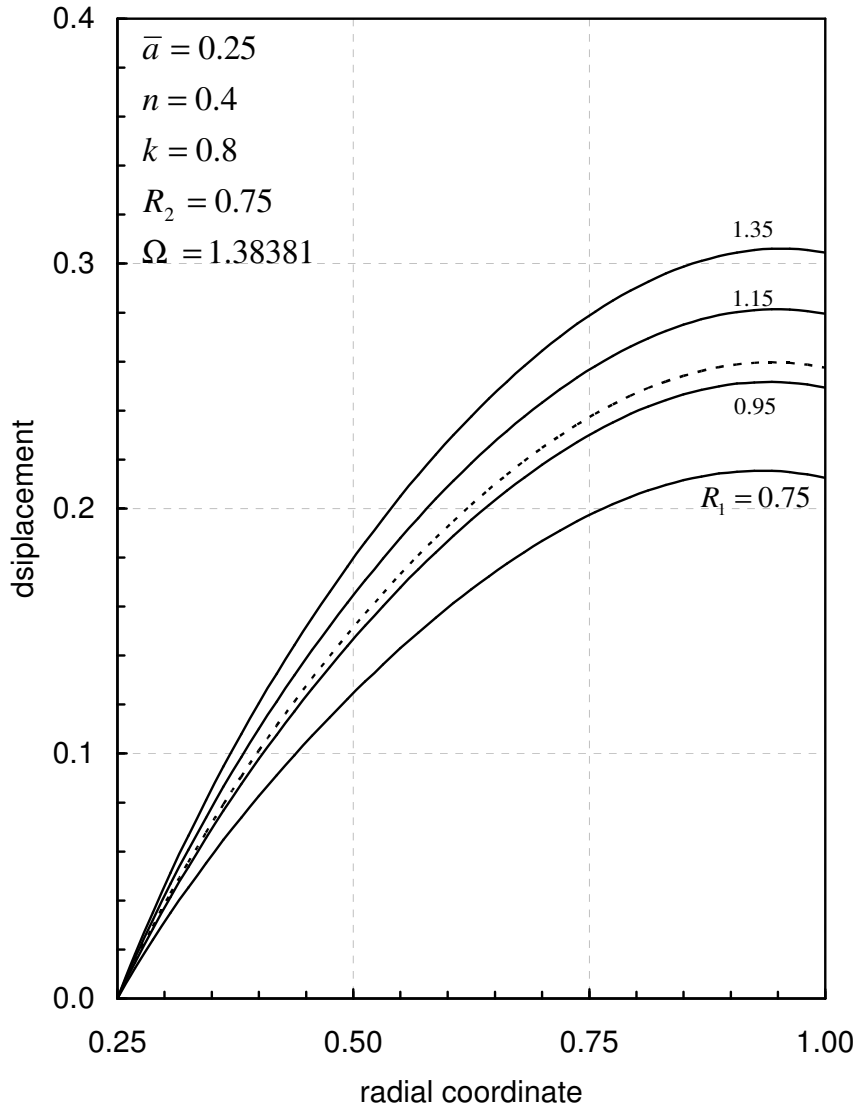

Figure 4.6 Effect of elastic orthotropy parameter R_1 on displacement for rotating annular disk with rigid inclusion.

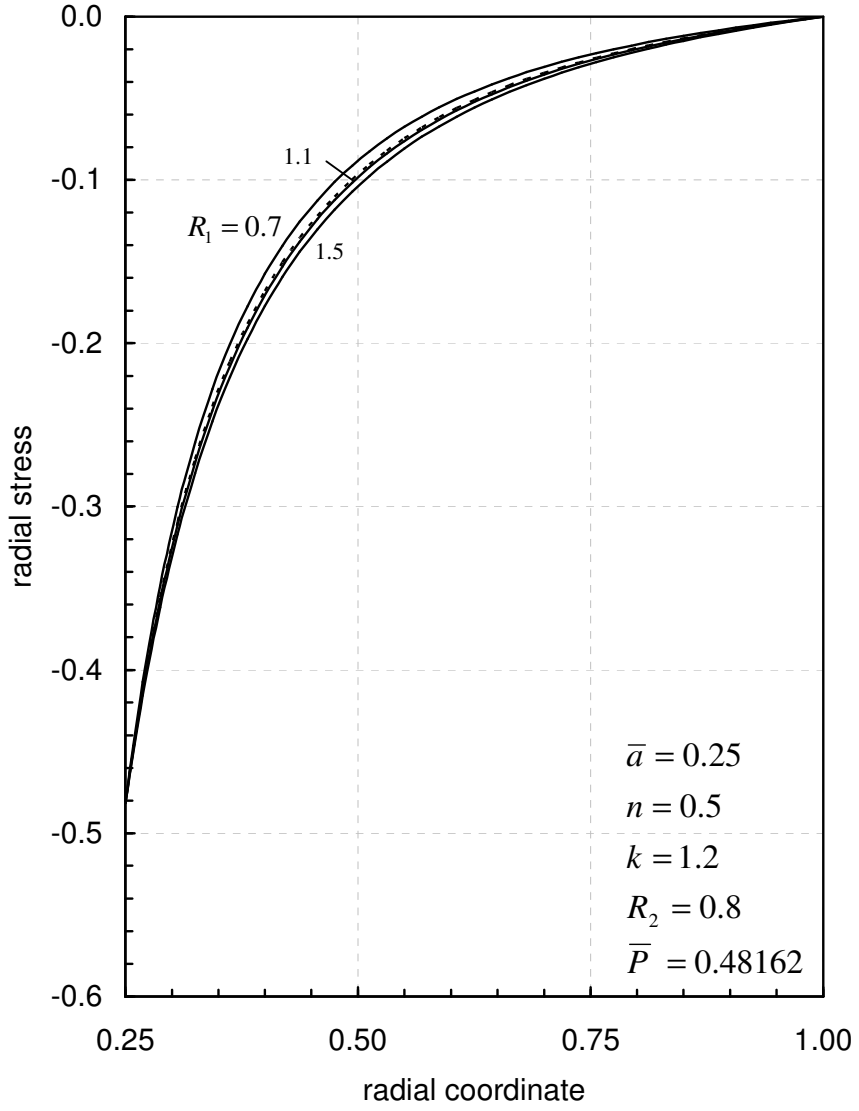

Figure 4.7 Effect of elastic orthotropy parameter R_1 on radial stress distribution for stationary annular disk subjected to internal pressure.

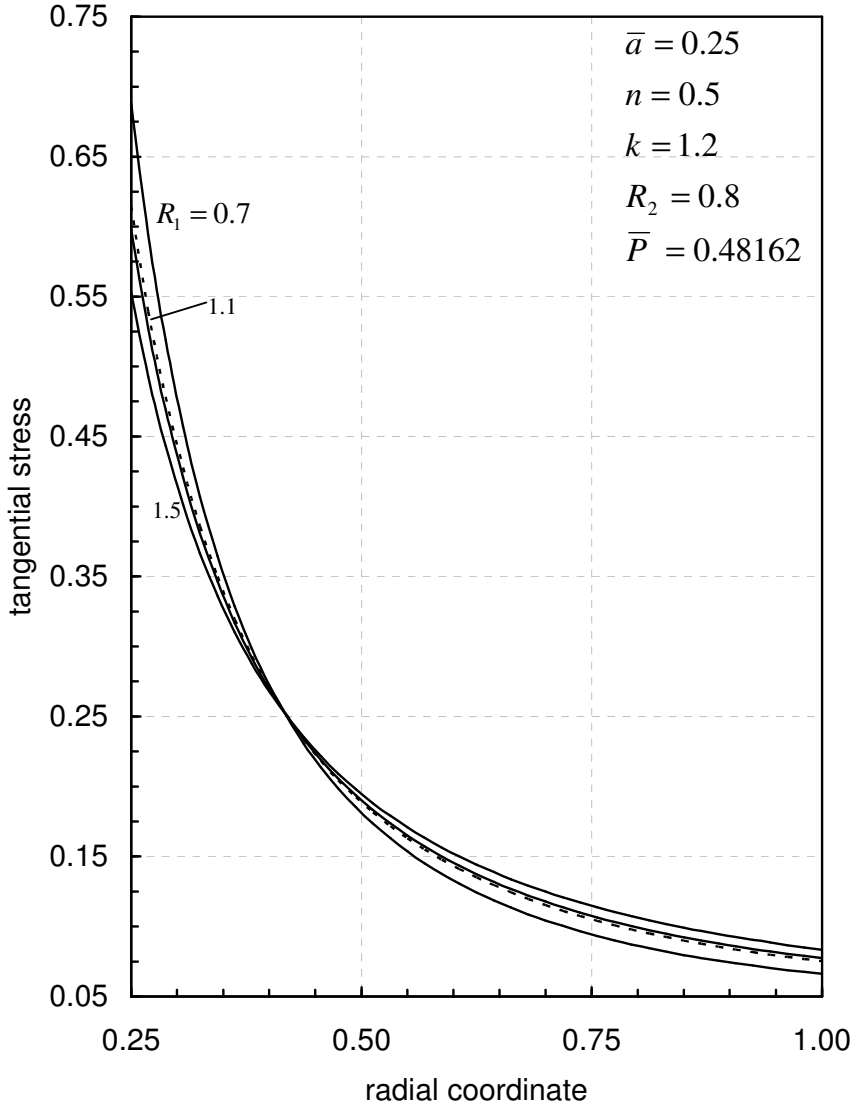

Figure 4.8 Effect of elastic orthotropy parameter R_1 on circumferential stress distribution for stationary annular disk subjected to internal pressure.

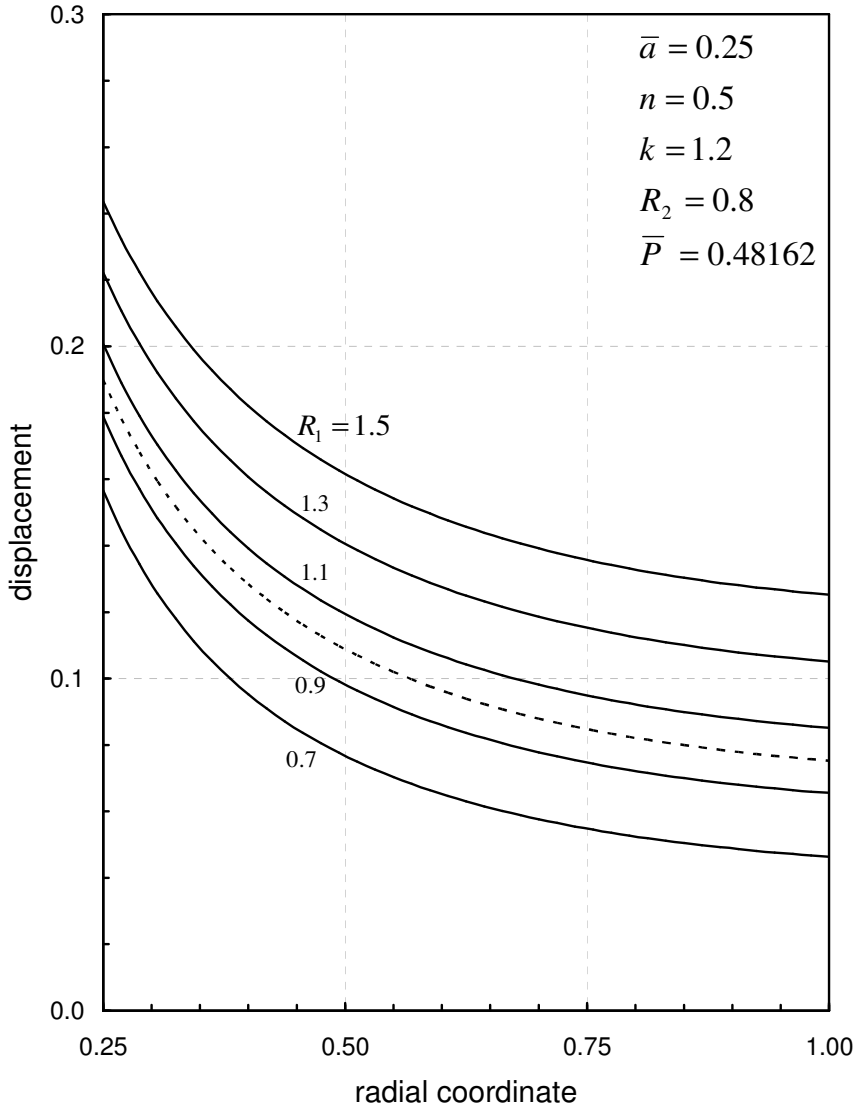

Figure 4.9 Effect of elastic orthotropy parameter R_1 on displacement for stationary annular disk subjected to internal pressure.

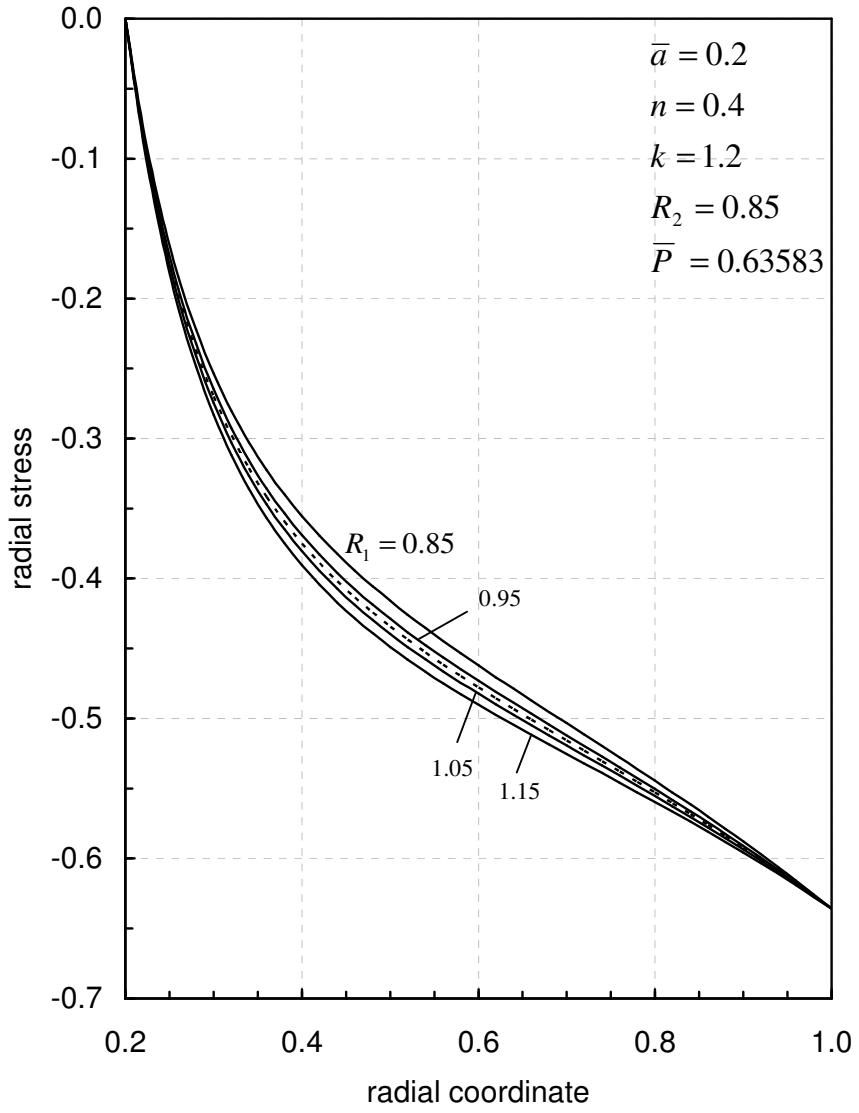

Figure 4.10 Effect of elastic orthotropy parameter R_1 on radial stress distribution for stationary annular disk subjected to external pressure.

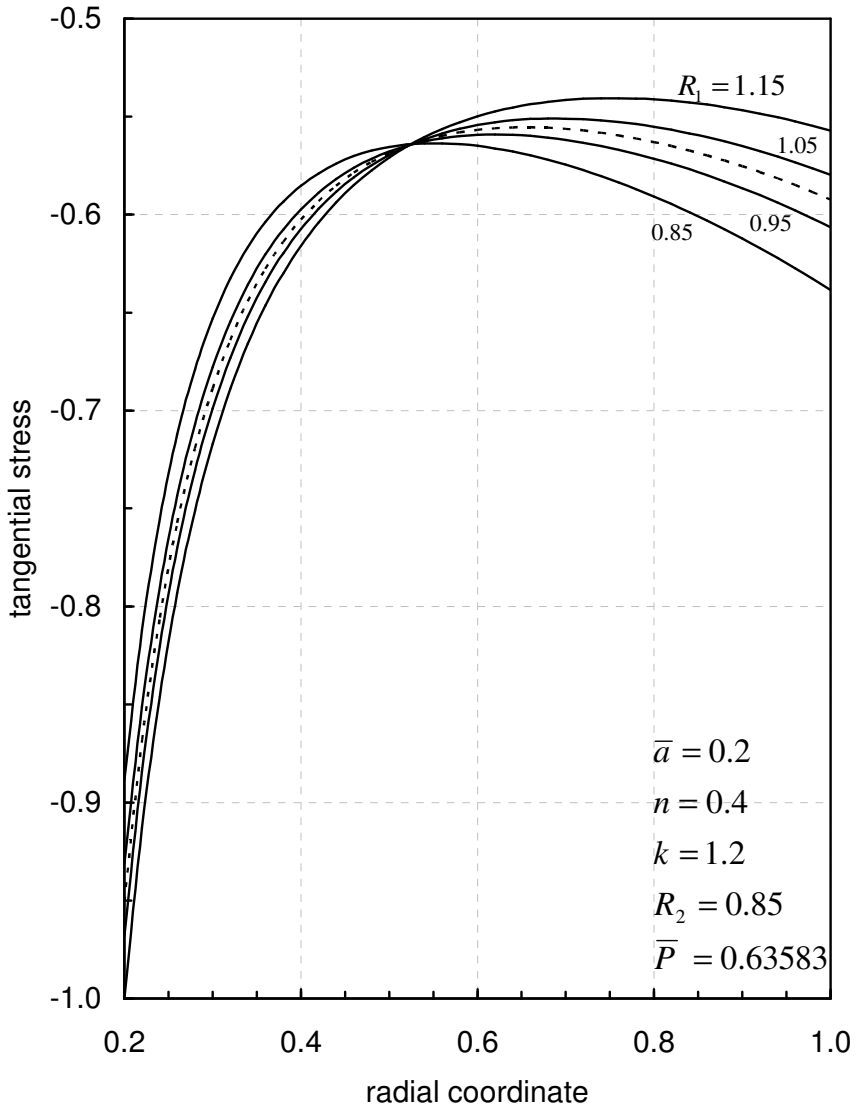

Figure 4.11 Effect of elastic orthotropy parameter R_1 on circumferential stress distribution for stationary annular disk subjected to external pressure.

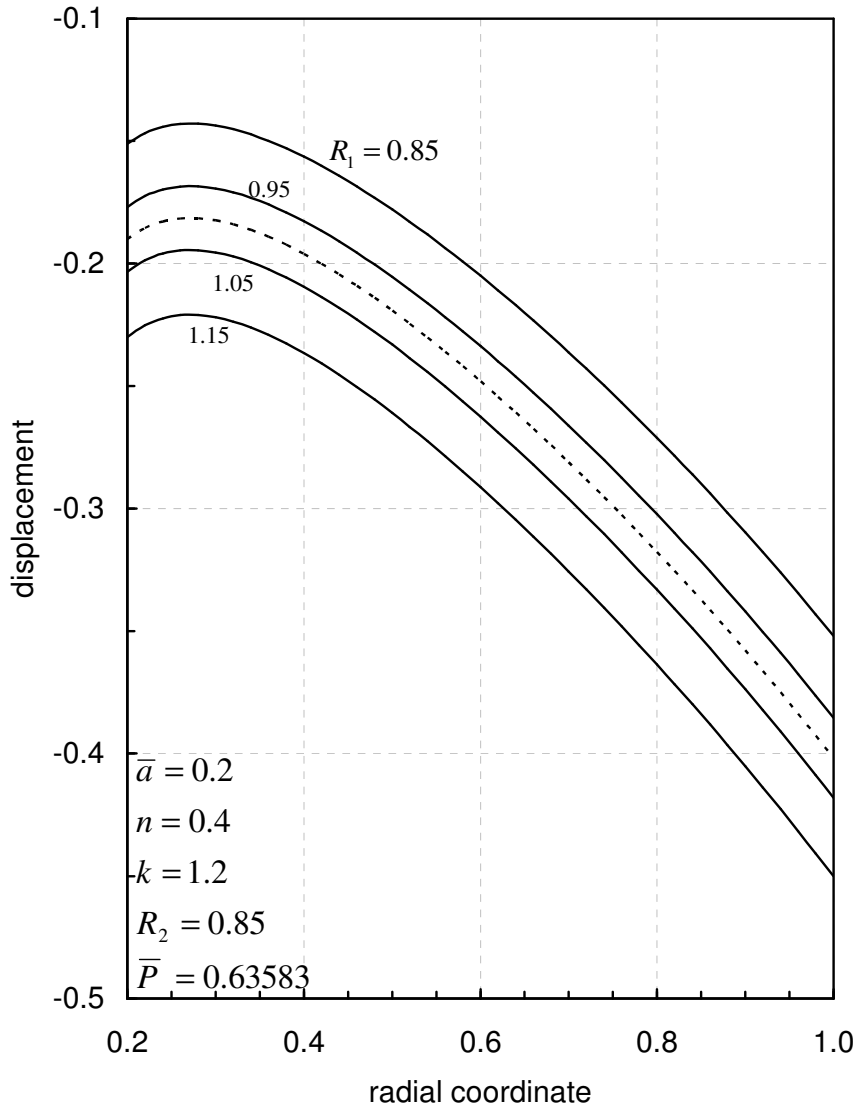

Figure 4.12 Effect of elastic orthotropy parameter R_1 on displacement for stationary annular disk subjected to external pressure.

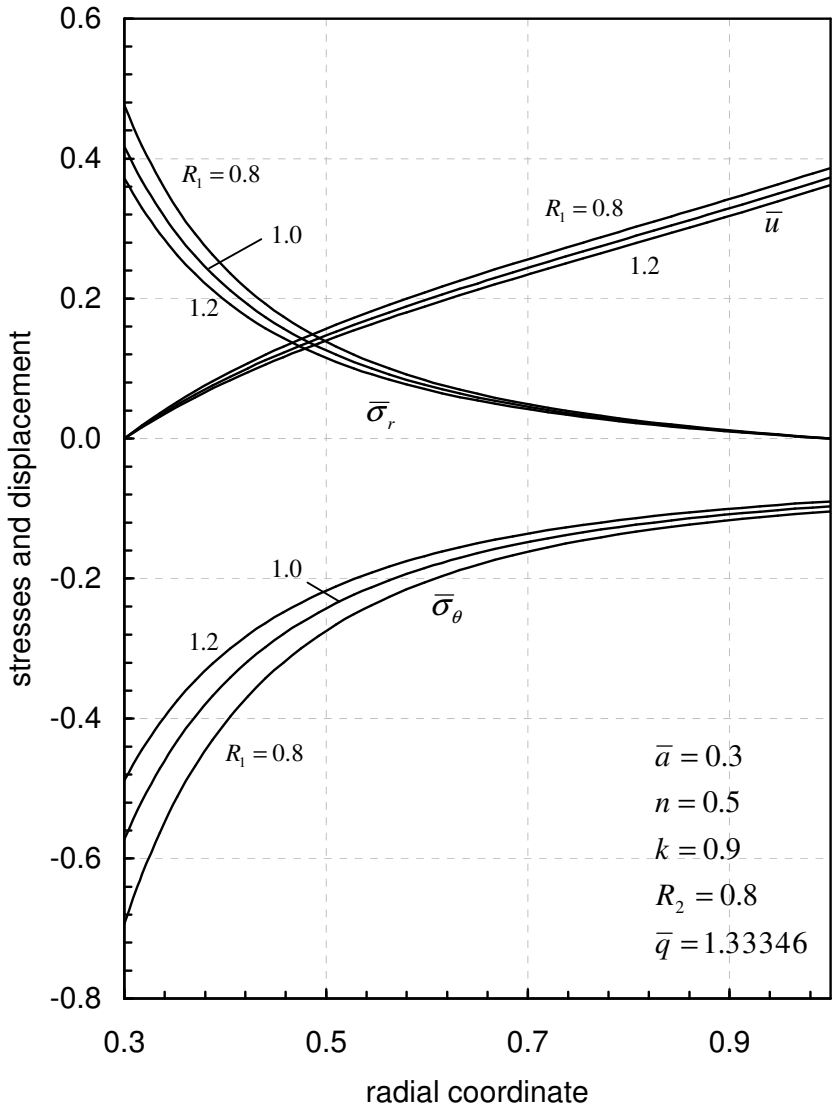

Figure 4.13 Effect of elastic orthotropy parameter R_1 on stress and displacement distributions for stationary annular disk with rigid inclusion under the thermal load.

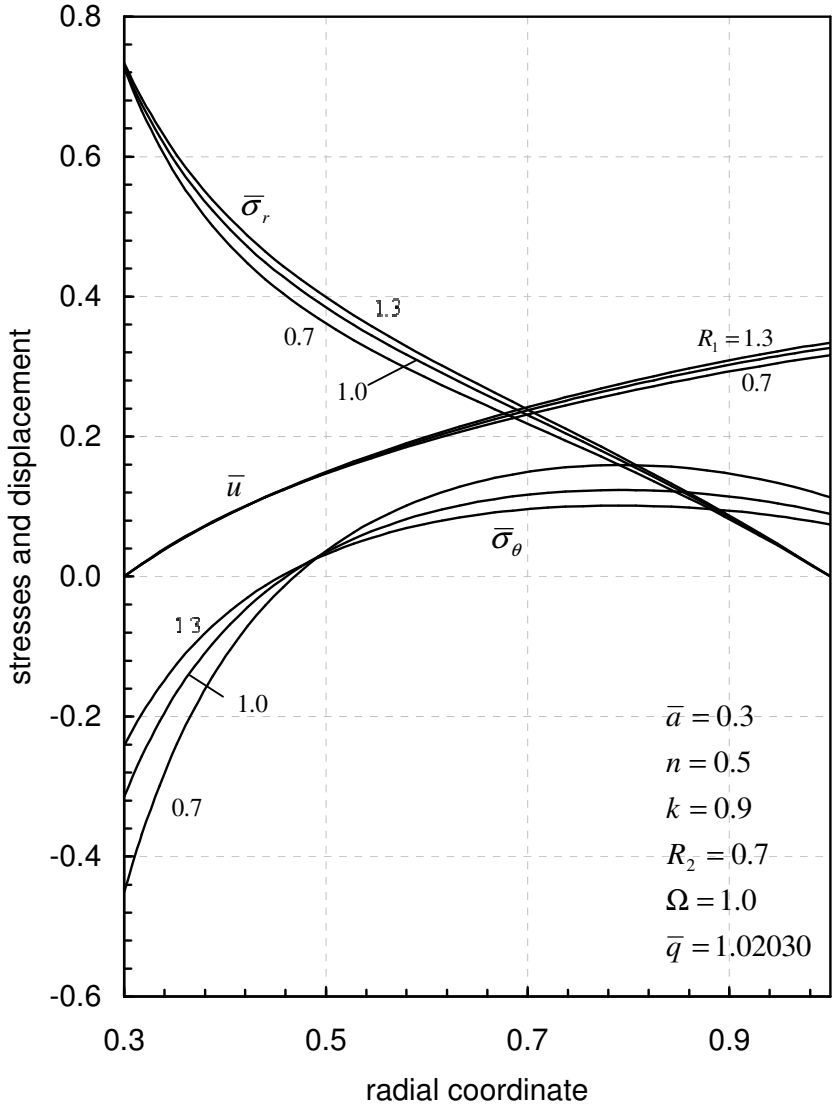

Figure 4.14 Effect of elastic orthotropy parameter R_1 on stress and displacement distributions for rotating annular disk with rigid inclusion under the thermal load.

4.2 Elastic-Plastic Numerical Solutions

Fig. (4.15) shows that the propagation of elastic-plastic border radius with increasing angular speed , for a rotating solid disk. It is seen from that, the size of plastic region decreases with increasing values of parameter R_2, except small angular speeds. Figures (4.16)-(4.17) show the effect of parameter R_2 on the stress, strain and radial displacement. It is seen from Fig. (4.17) that, the plastic strains and radial displacement decrease for increasing values of parameter R_2. It appears that the axial plastic strain is strongly affected by the parameter R_2, but, the effect of parameter R_2 on the plastic stresses is very slight. Fig.(4.18) shows that the effect of parameter R_2 on the residual stresses and the radial displacement for a rotating solid disk. Fig.(4.18) shows that the effect of parameter R_2 on the residual stresses are very slight. However, the residual tensile circumferential stress at the outer surface decreases with increasing values of parameter R_2. It is also seen from Fig. (4.18) that, the residual radial displacement decreases with increasing values of parameter R_2. The effect of parameter R_2 on the variation of residual radial displacement is significant.

Figures (4.19) and (4.20) show the propagation of elastic-plastic border radius with increasing angular speed, for a free rotating annular disk. It is seen from Fig.(4.19) and Fig. (4.20) that, in general, for sufficiently high angular speeds the size of plastic region decreases with increasing values of parameters R_1 and R_2. Figures (4.21)-(4.22) show the effect of parameter R_1 and R_2 on the stress, strain and radial displacement distributions, for a free rotating annular disk. The increase of radial displacement is significant, but the radial stress varies slightly. In addition, it is seen from Fig (4.21), the maximum increases for the circumferential stress and plastic strains occur at the inner surface. Fig. (4.23) shows that the effect of parameter R_1 on the residual stresses and the radial

displacement for a free rotating annular disk. It can be seen from Fig. (4.23), the effect of parameter R_1 on the residual stresses is very small. When the value of parameter R_1 increases, the residual radial displacement increases slightly. Fig. (4.24) shows that the effect of parameter R_2 on the residual stresses and the radial displacement, for a free rotating annular disk. It is seen from Fig. (4.24) that, the effect of parameter R_2 on the residual stresses at regions near the inner surface is very slight. The magnitude of residual circumferential stress is affected by the parameter R_2, the variation of residual radial stress is slight. The residual radial displacement and the maximum residual tensile circumferential stress decrease with increasing values of parameter R_2. In addition, at regions near the outer surface the magnitude of residual tensile circumferential stress decreases with increasing the values of parameter R_2 and the location of maximum residual tensile circumferential stress moves toward to the outer surface with decreasing values of parameter R_2. It also noted that the magnitude of maximum residual tensile circumferential stress is affected by the variation of parameter R_2, but the variation of maximum residual compressive stress is slight. The residual tensile circumferential stress at the outer surface decreases with increasing values of parameter R_2.

Figures (4.25) and (4.26) show propagation of elastic-plastic border radius with increasing angular speed, for a rotating disk with rigid inclusion. It is seen from Fig. (4.25) and (4.26) that, in general, in sufficiently high angular speeds the size of plastic region decreases with increasing values of parameters R_1 and R_2. Figures (4.27)-(4.30) show the effect of parameters R_1 and R_2 on the residual stresses and radial displacement, for a rotating disk with rigid inclusion. Compared to R_1 , the effect of R_2 is more significant. As observed from Fig. (4.31) that, when the value of parameter R_1 increases, the residual stresses and the radial displacement increase, but the residual circumferential

stress at the near outer surface decreases. Fig. (4.32) shows that, when the value of parameter R_2 increases, the residual circumferential stresses increase, but the variation of maximum residual radial stress is very small and the residual radial displacement decreases significantly. It is seen from Figures (4.31) and (4.32) that, the location of maximum residual tensile circumferential stress moves toward the outer surface with decreasing values of parameters R_1 and R_2.It is additionally observed that, the tensile circumferential stress can change its sign in the small region with decreasing values of parameters R_1 and R_2, but the change of sign is more sensitive to parameter R_1.

Figures (4.33)-(4.38) show the effects of parameters R_1 and R_2 on stress, strain, displacement distributions for disk subjected to internal pressure. It can be observed from the figures that the effect of parameters R_1 and R_2 is not very significant for the internal pressure case.

Fig. (4.39) and Fig.(4.40) show the propagation of elastic-plastic border radius with increasing angular speed for stationary annular disk subjected to external pressure. Figures (4.41)-(4.44) show the effect of parameters R_1 and R_2 on the tress, strain, displacement, and residual stress distributions. It is seen from the figures, effect of parameter R_1 is more significant on displacement and residual stresses.

The thermal loading for rotating disk with rigid inclusion case is also considered. It is seen from Figures (4.45)-(4.48), in this case, stresses and strains are highly affected by the variation of the orthotropy parameters R_1 and R_2.

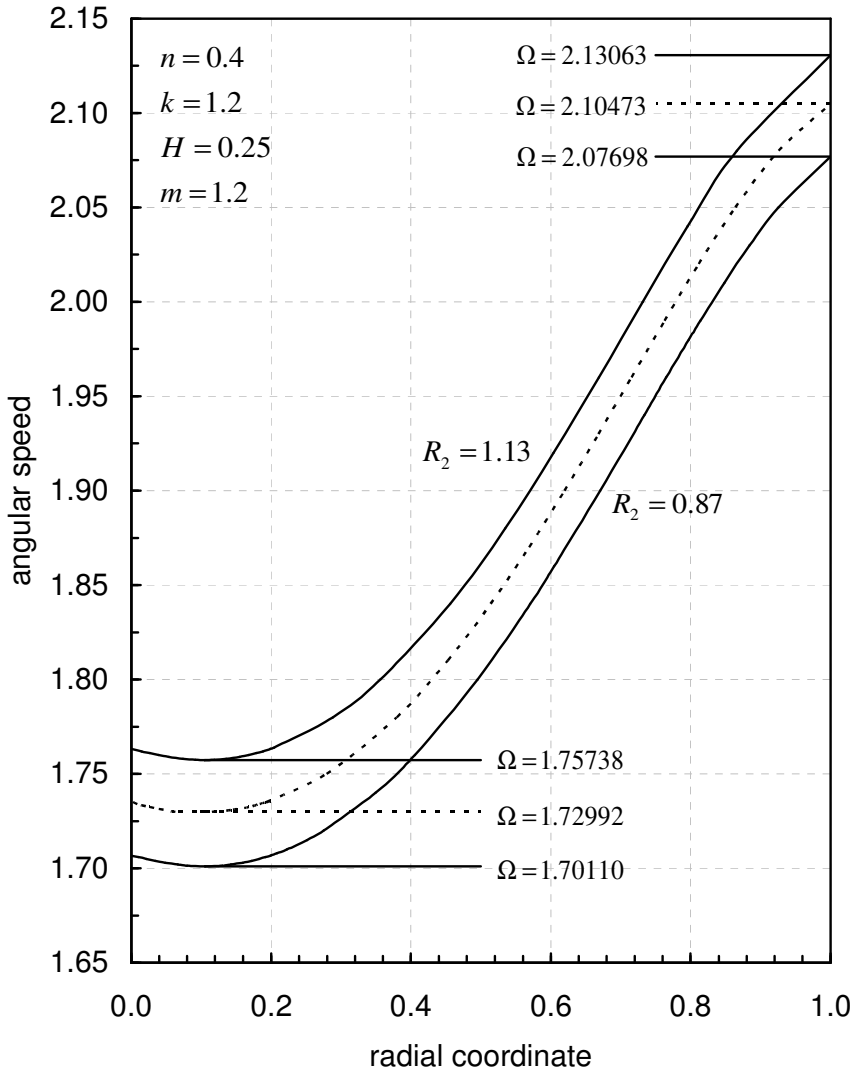

Figure 4.15 Propagation of elastic-plastic border radius with increasing angular speed due to effect of plastic orthotropy parameter R_2 for rotating solid disk.

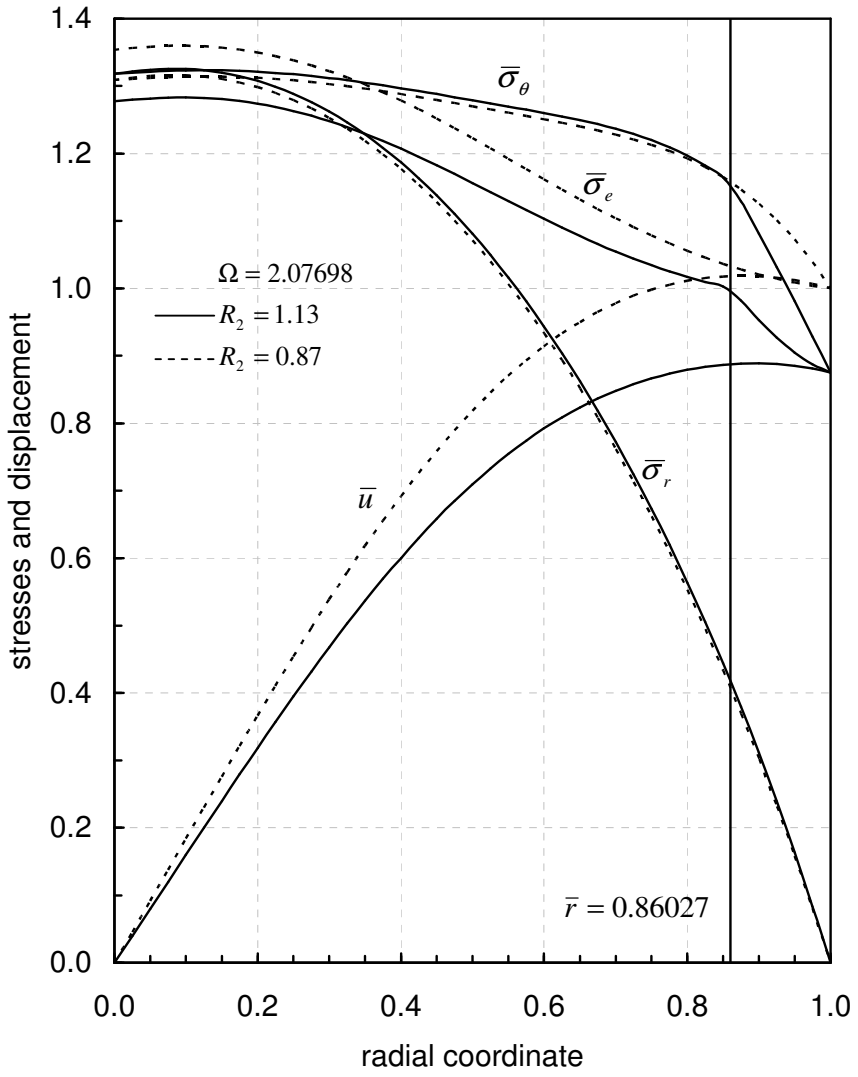

Figure 4.16 Effect of plastic orthotropy parameter R_2 on stresses and radial displacement distributions for rotating solid disk.

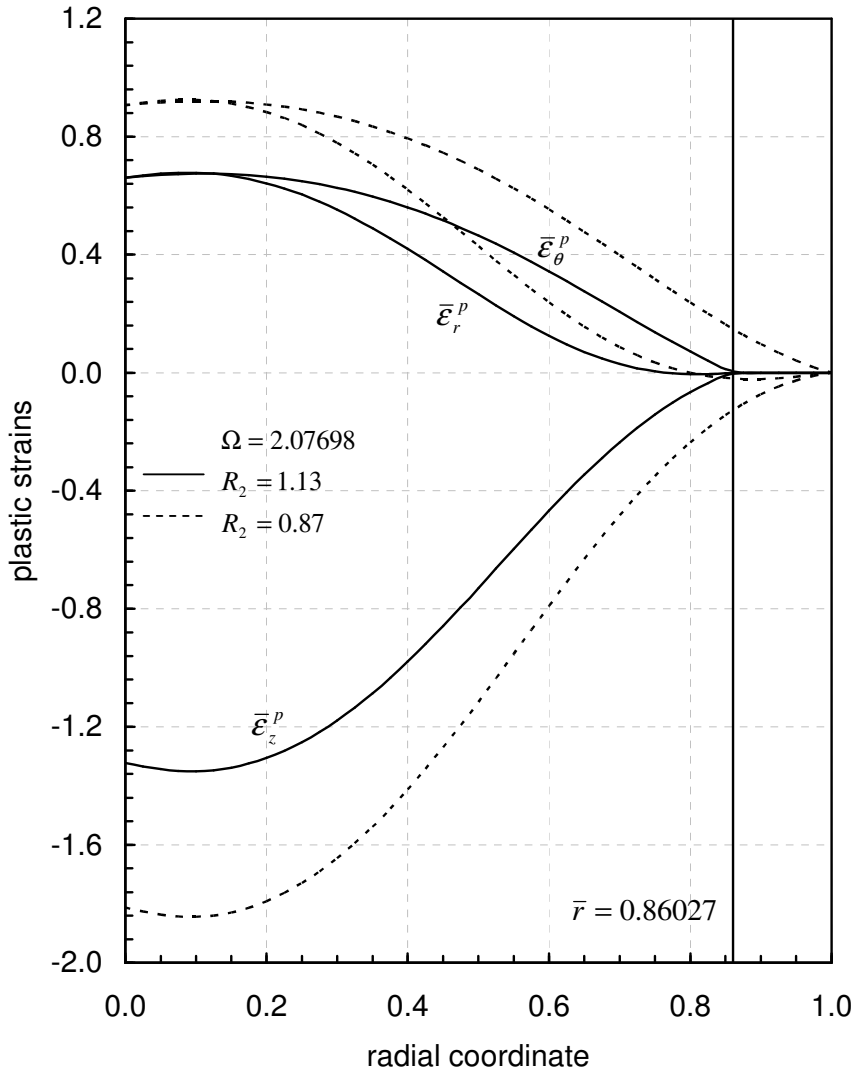

Figure 4.17 Effect of plastic orthotropy parameter R_2 on strains for rotating solid disk.

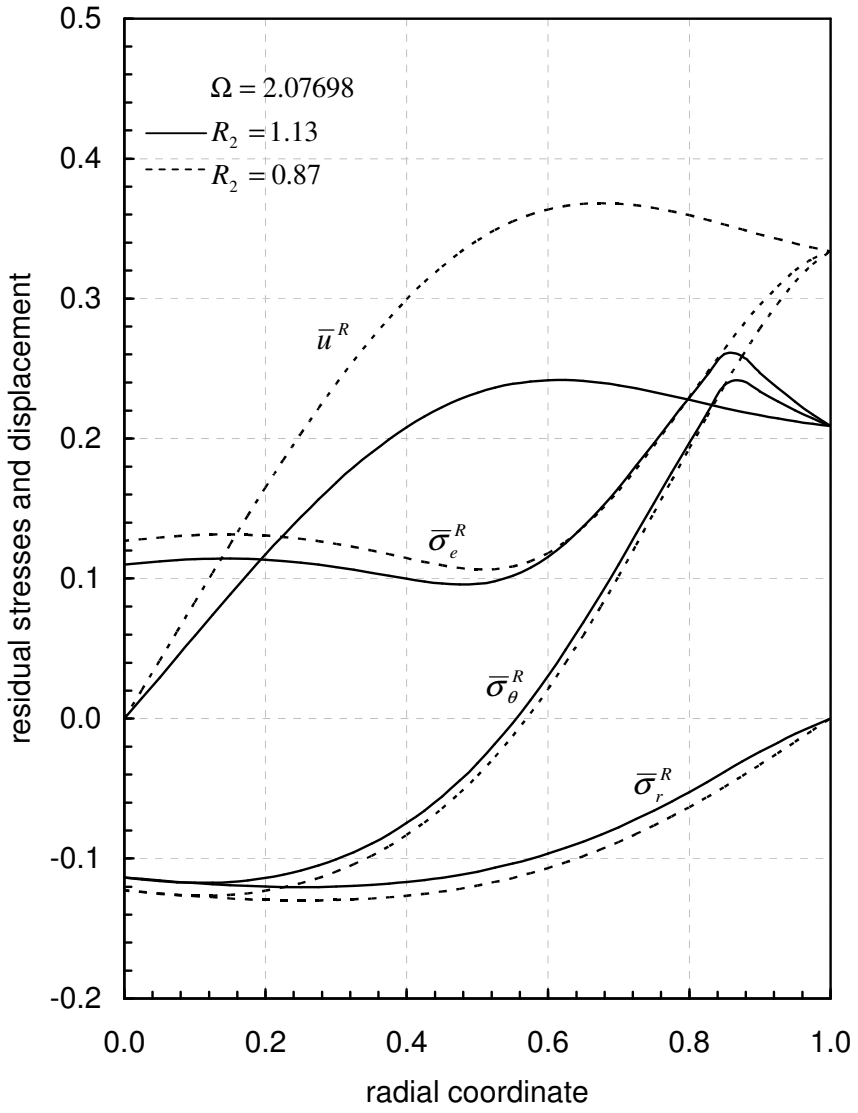

Figure 4.18 Effect of plastic orthotropy parameter R_2 on residual stress distributions for rotating solid disk.

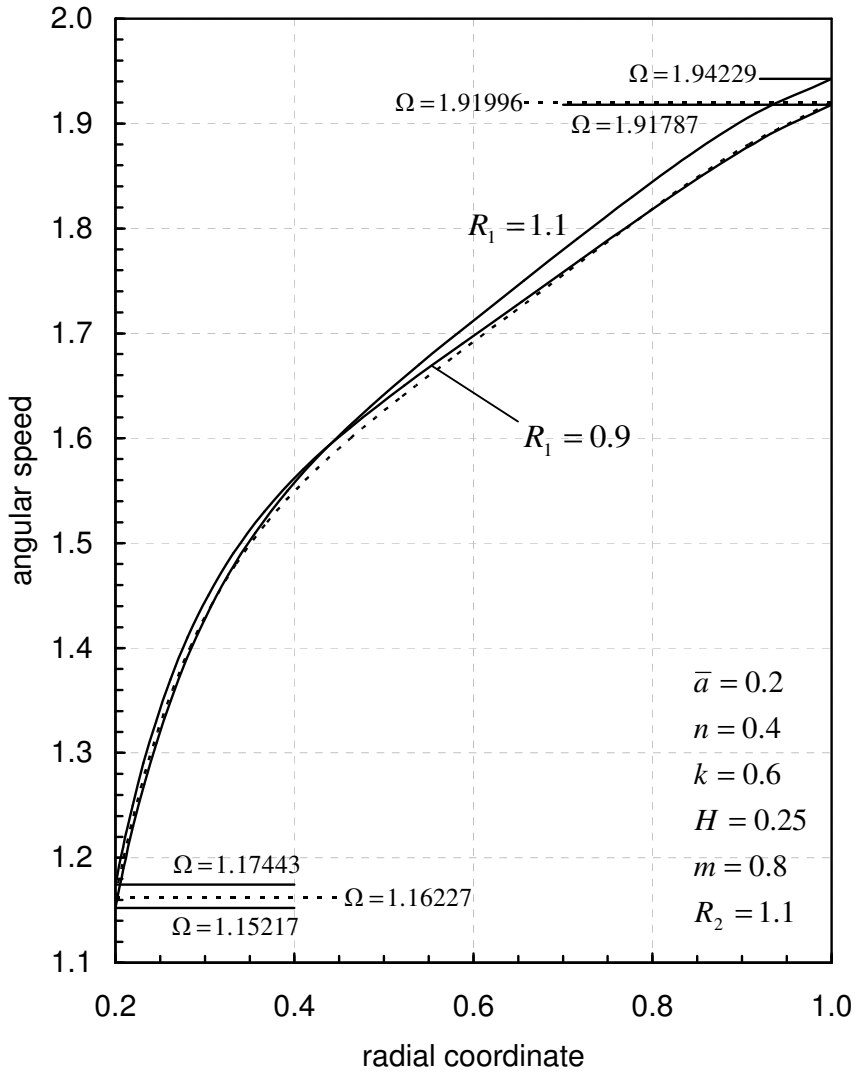

Figure 4.19 Propagation of elastic-plastic border radius with increasing angular speed due to effect of elastic orthotropy parameter R_1 for rotating annular disk.

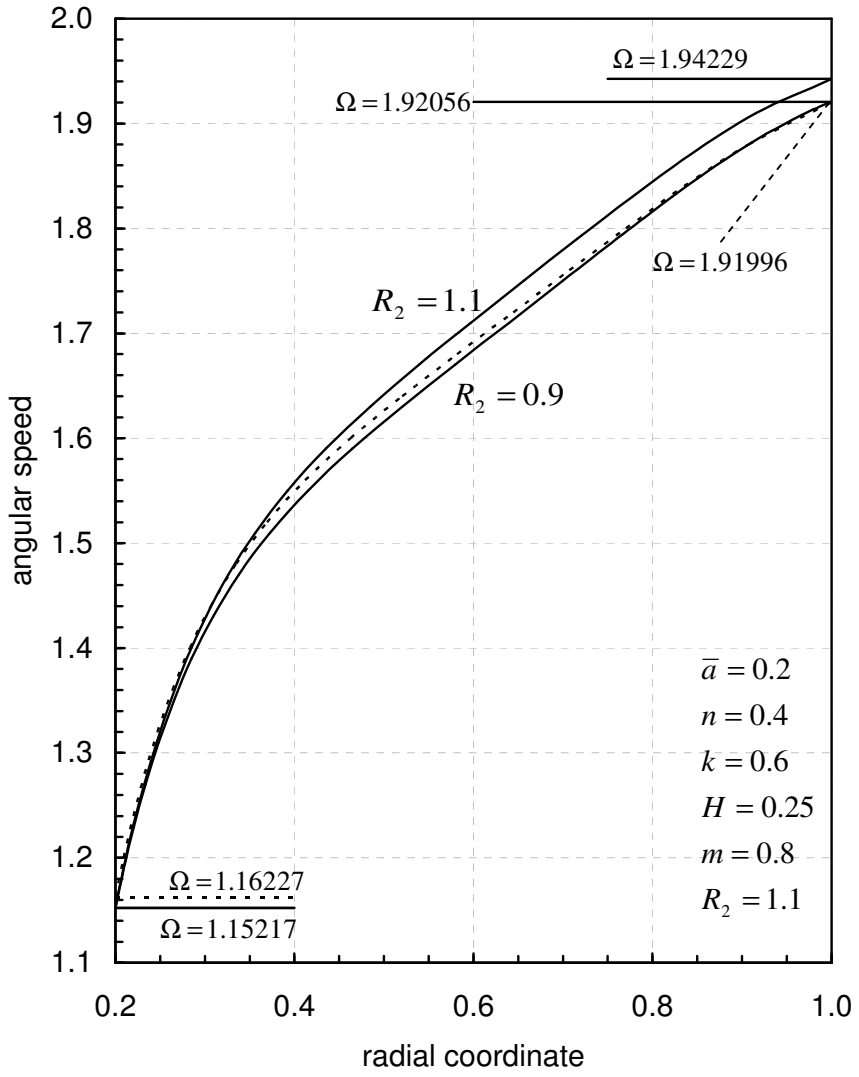

Figure 4.20 Propagation of elastic-plastic border radius with increasing angular speed due to effect of plastic orthotropy parameter R_2 for rotating annular disk.

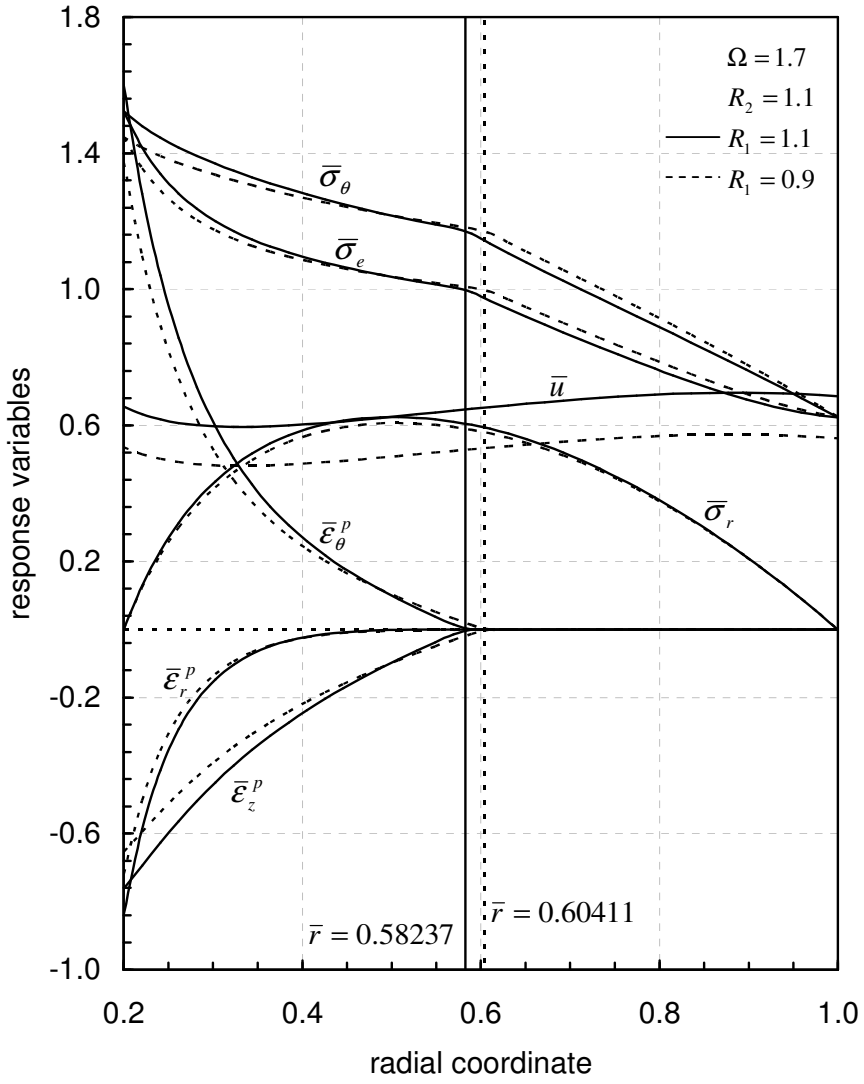

Figure 4.21 Effect of elastic orthotropy parameter R_1 on stress, strain and radial displacement distributions for rotating annular disk.

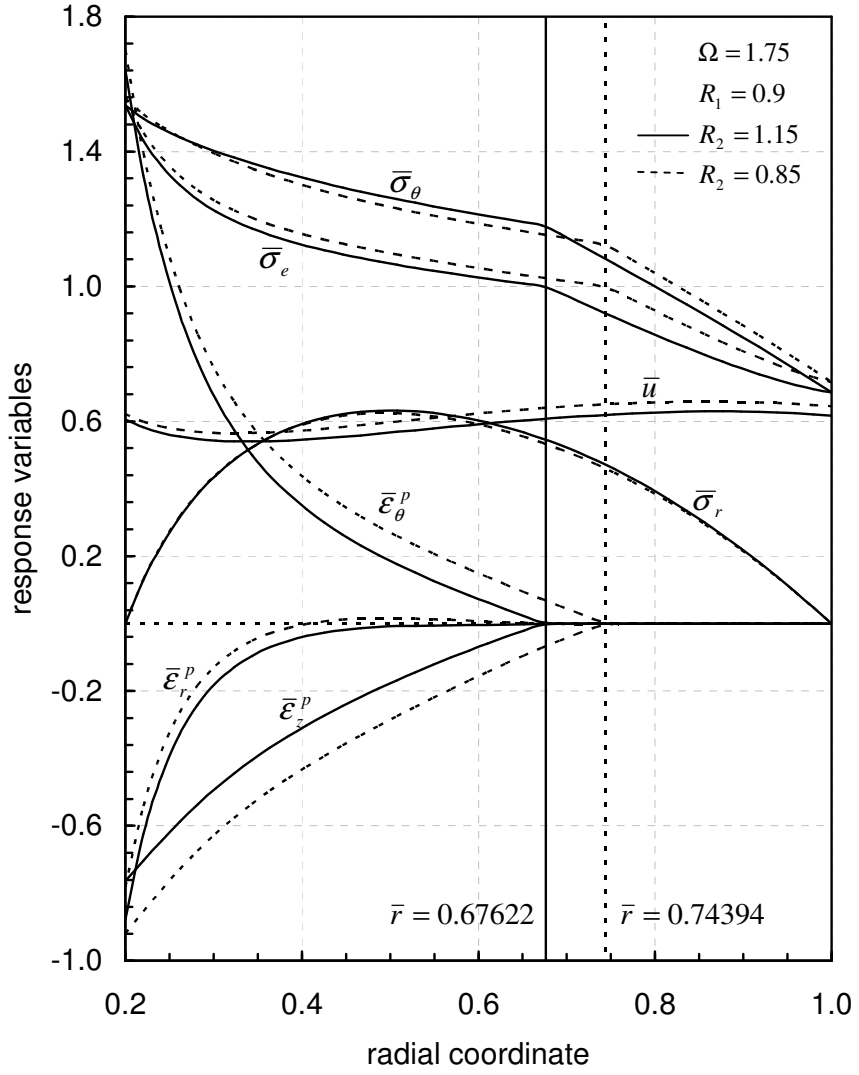

Figure 4.22 Effect of plastic orthotropy parameter R_2 on stress, strain and radial displacement distributions for rotating annular disk.

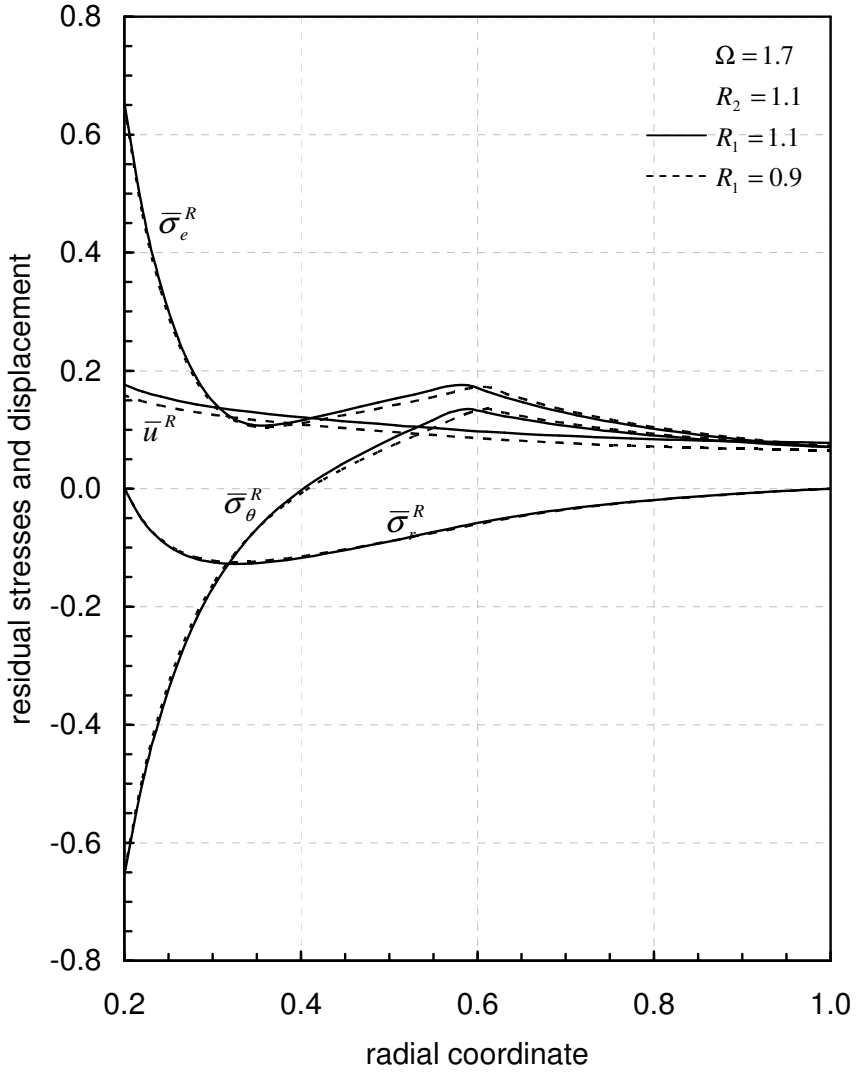

Figure 4.23 Effect of elastic orthotropy parameter R_1 on residual stress distributions for rotating annular disk.

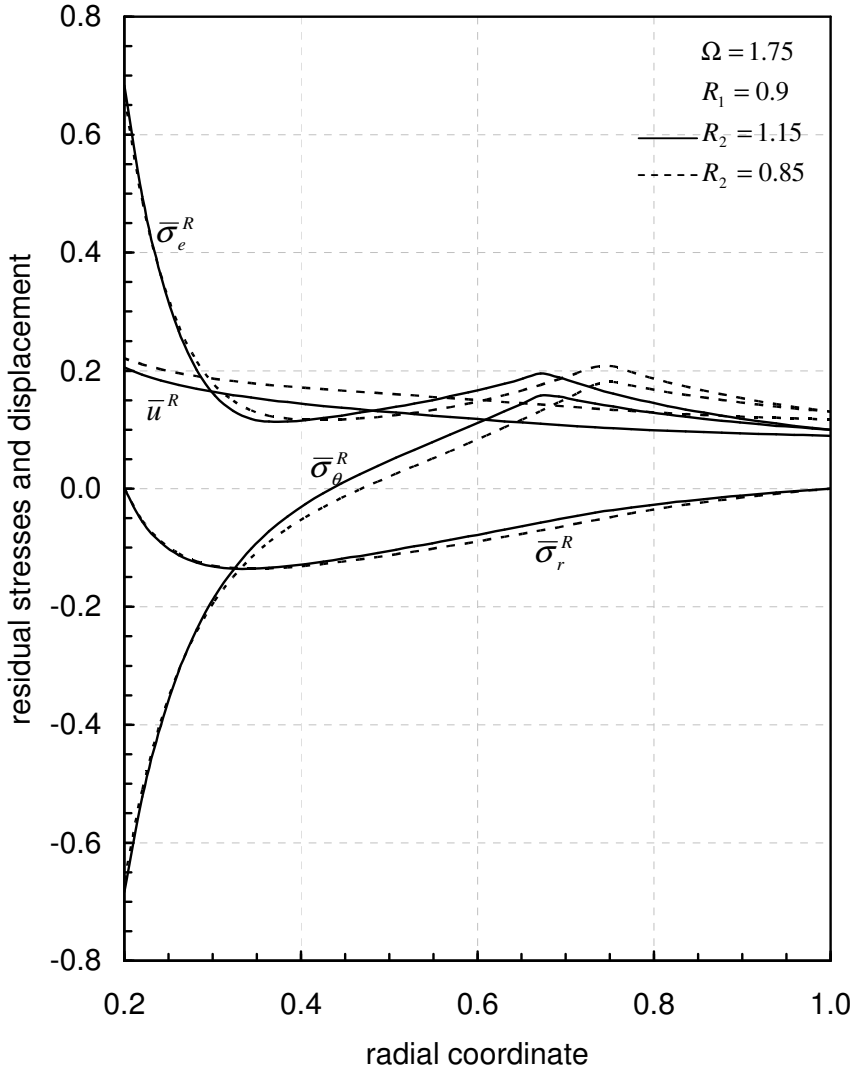

Figure 4.24 Effect of plastic orthotropy parameter R_2 on residual stress distributions for rotating annular disk.

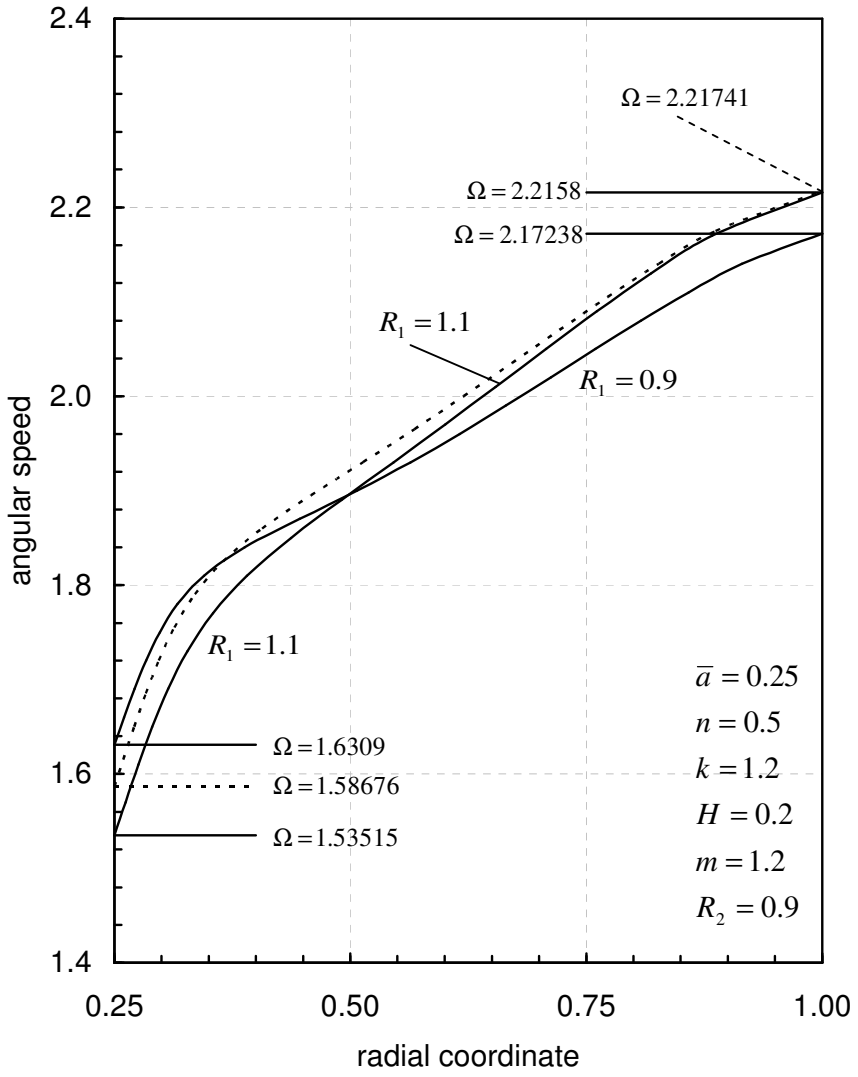

Figure 4.25 Propagation of elastic-plastic border radius with increasing angular speed due to effect of elastic orthotropy parameter R_1 for rotating disk with rigid inclusion.

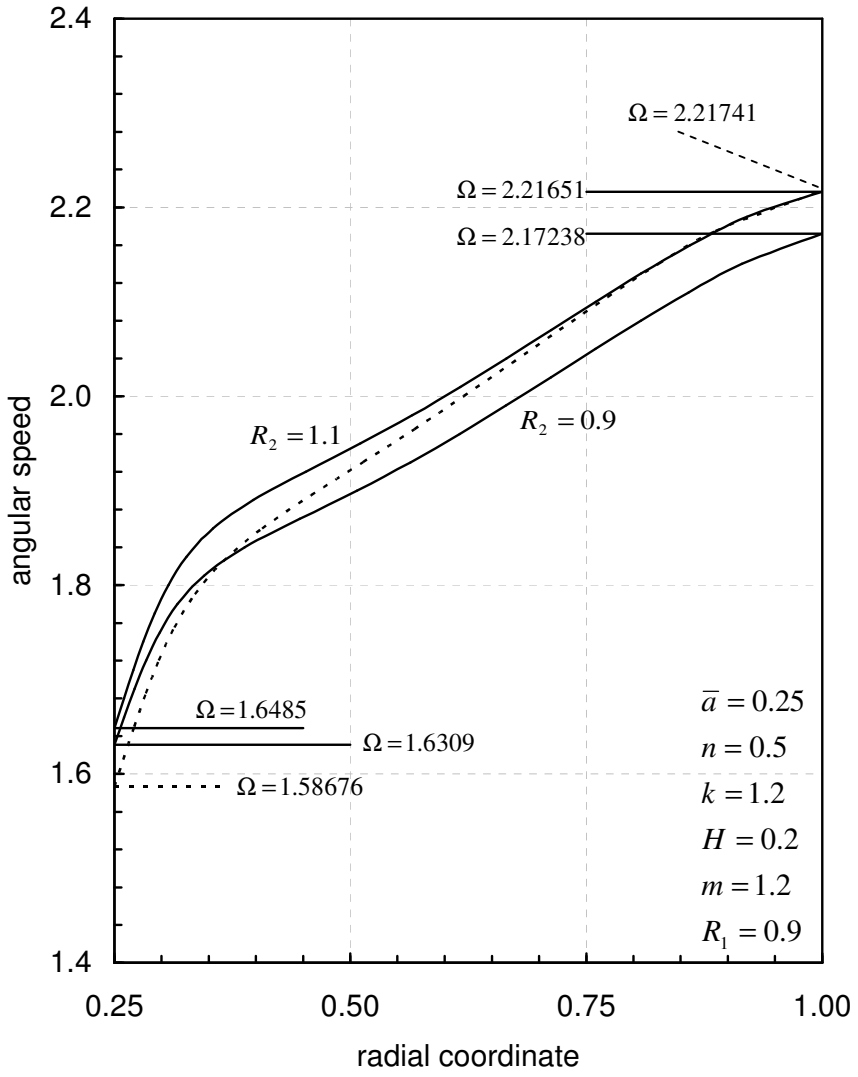

Figure 4.26 Propagation of elastic-plastic border radius with increasing angular speed due to effect of plastic orthotropy parameter R_2 for rotating disk with rigid inclusion.

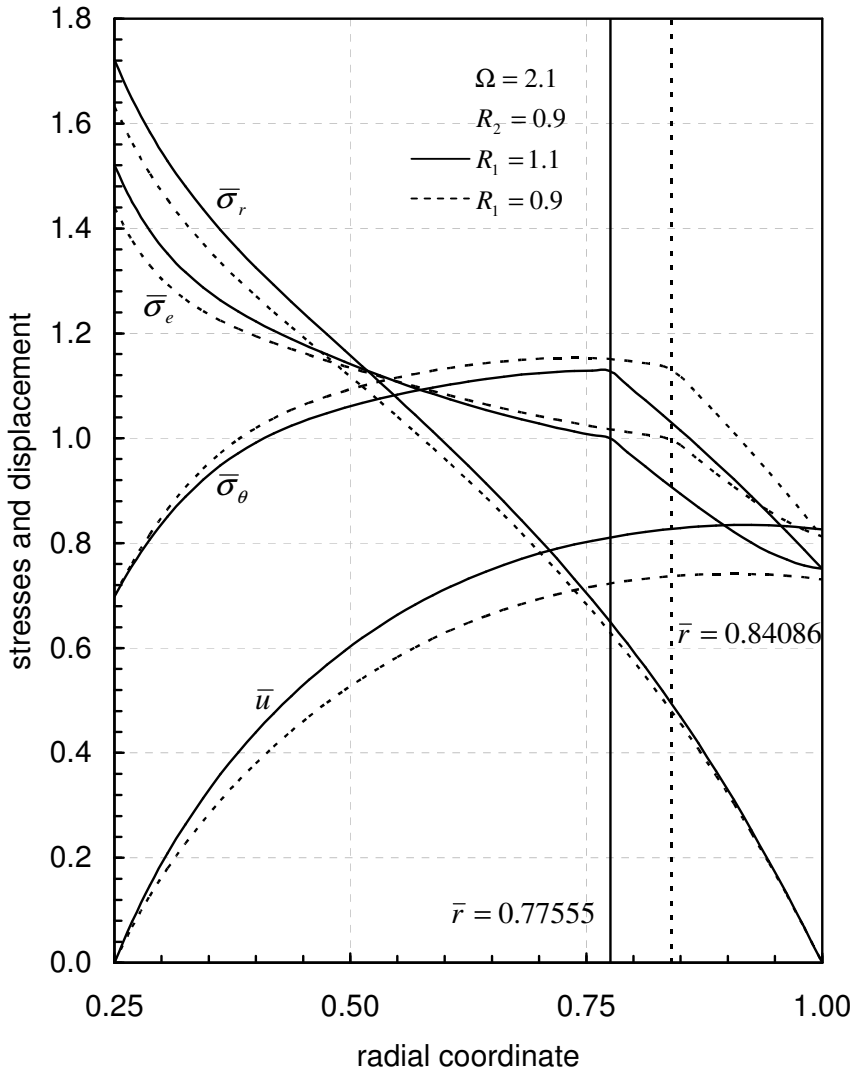

Figure 4.27 Effect of elastic orthotropy parameter R_1 on stress and radial displacement distributions for rotating disk with rigid inclusion.

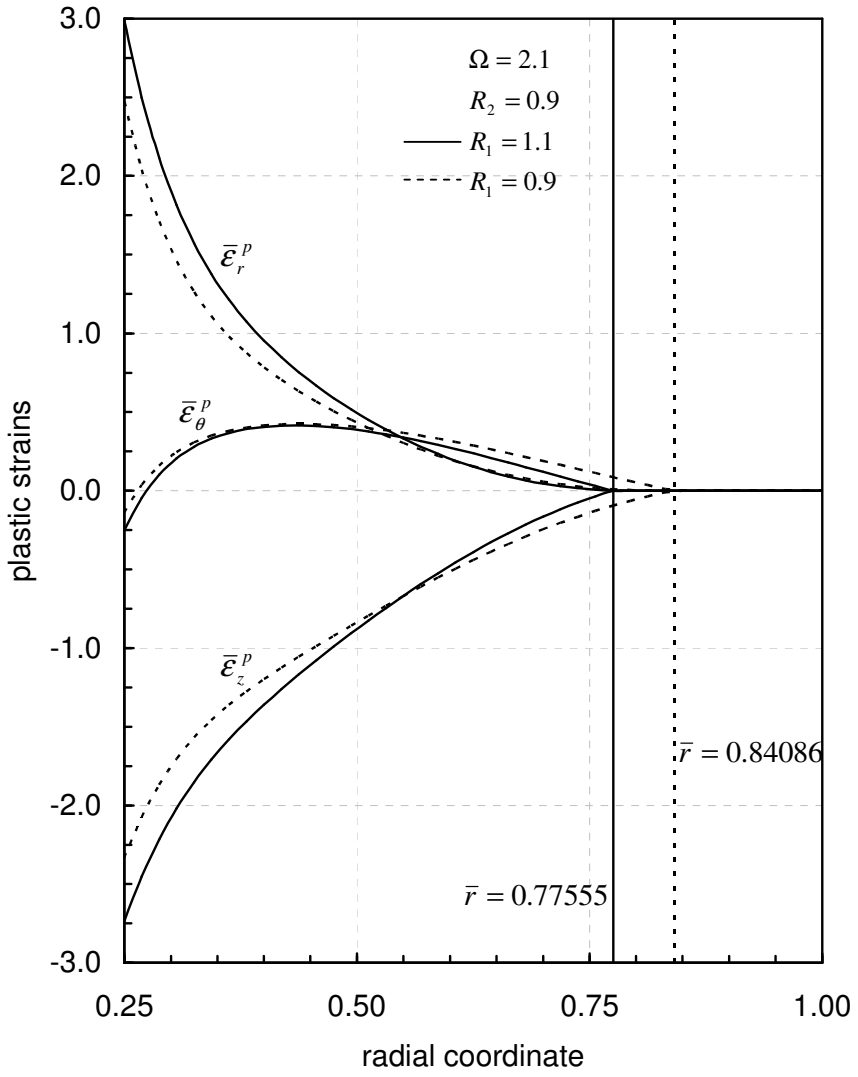

Figure 4.28 Effect of elastic orthotropy parameter R_1 on strains for rotating disk with rigid inclusion.

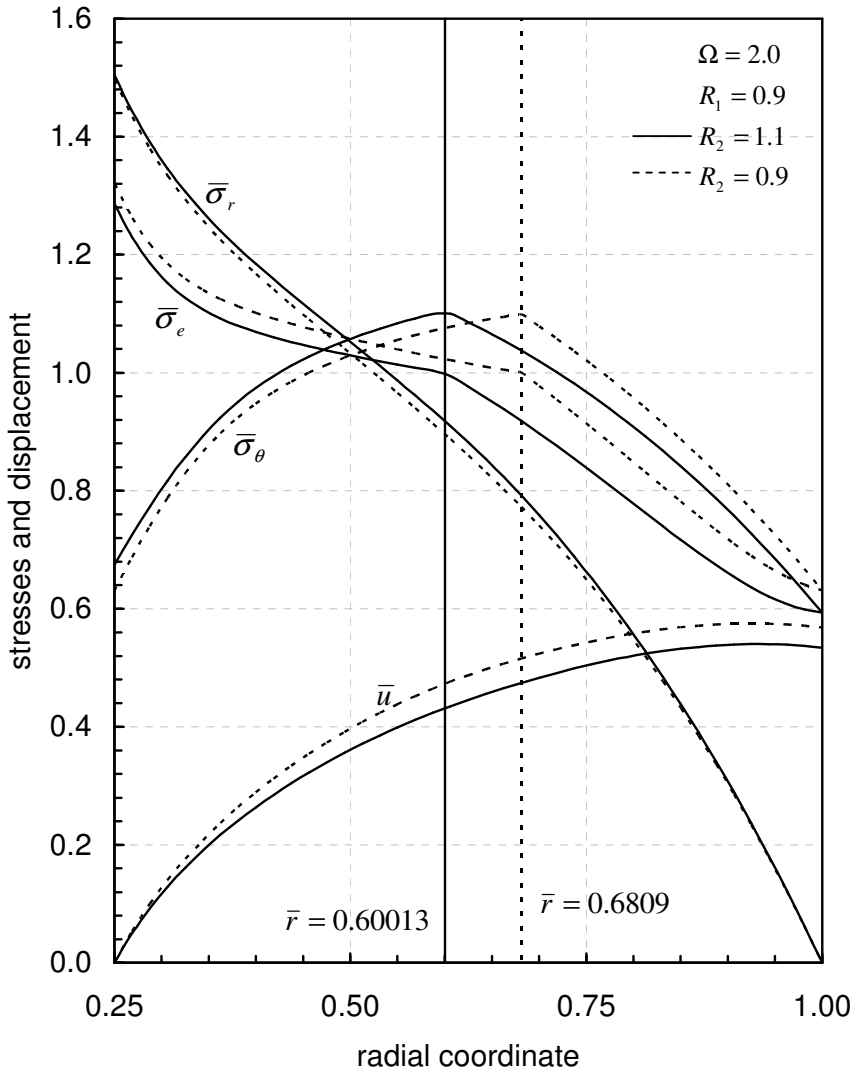

Figure 4.29 Effect of plastic orthotropy parameter R_2 on stress and radial displacement distributions for rotating disk with rigid inclusion.

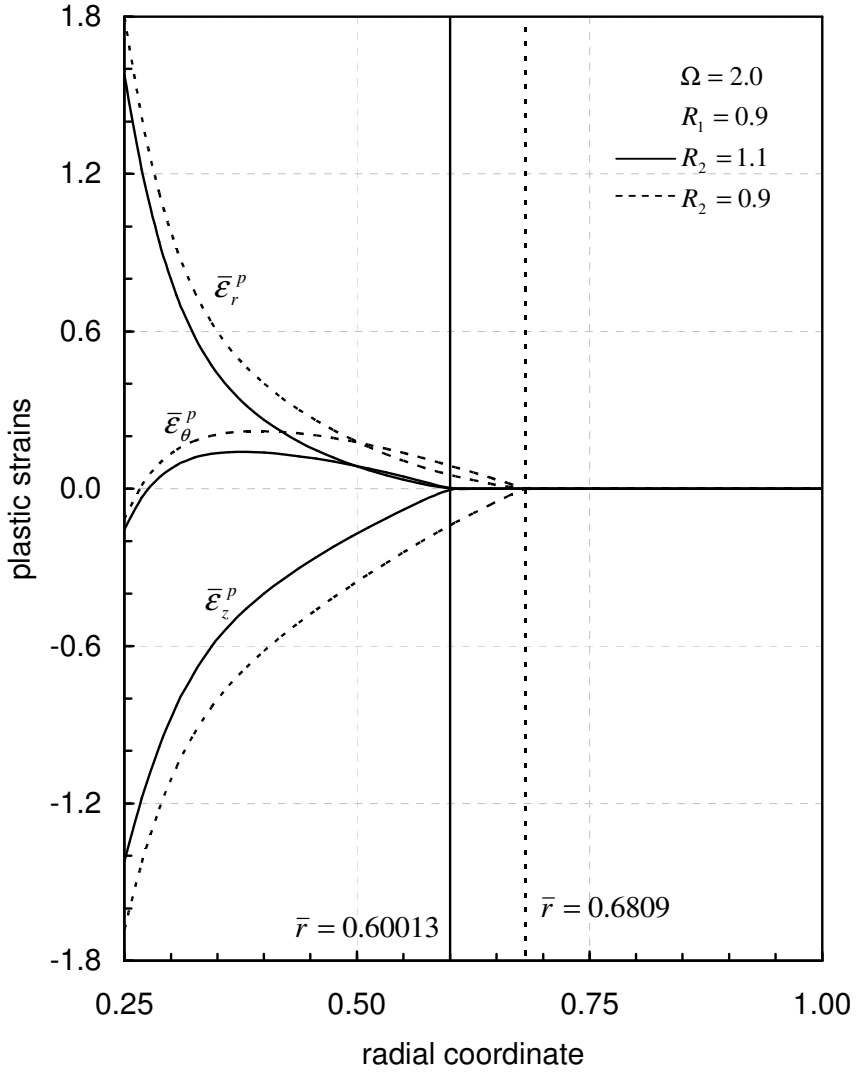

Figure 4.30 Effect of plastic orthotropy parameter R_2 on strains for rotating disk with rigid inclusion.

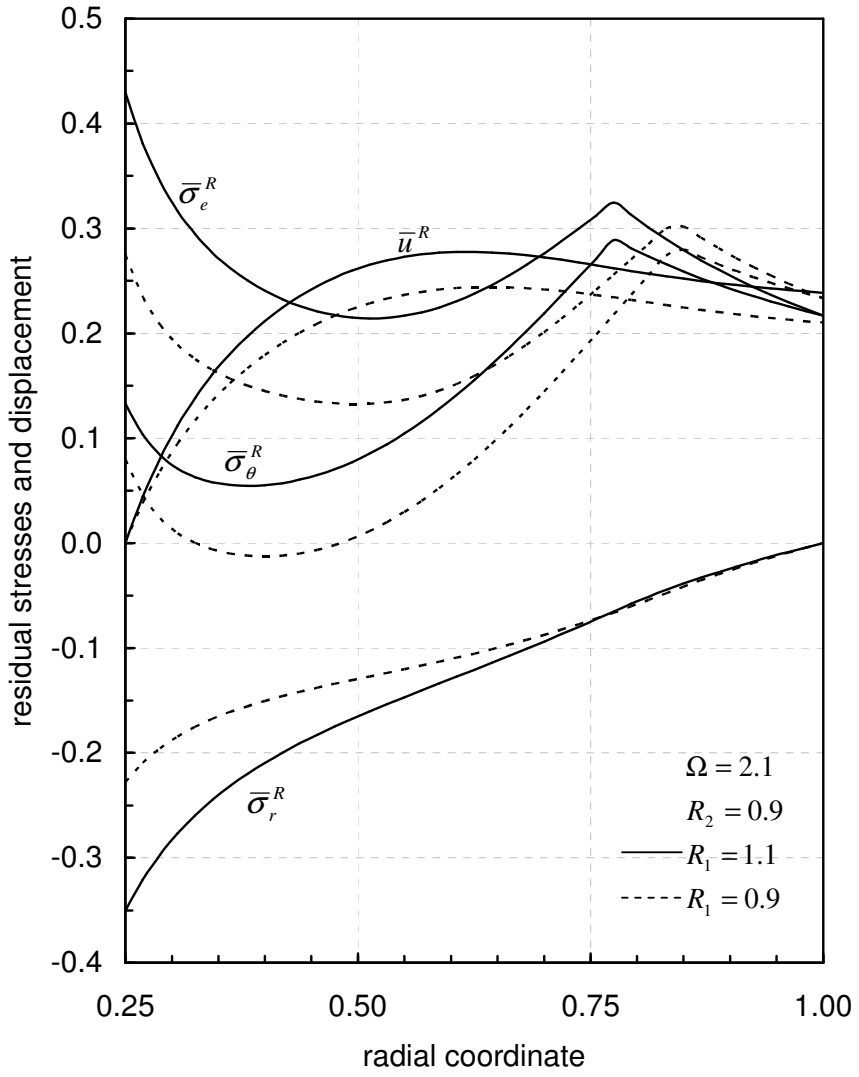

Figure 4.31 Effect of elastic orthotropy parameter R_1 on residual stress distributions for rotating disk with rigid inclusion.

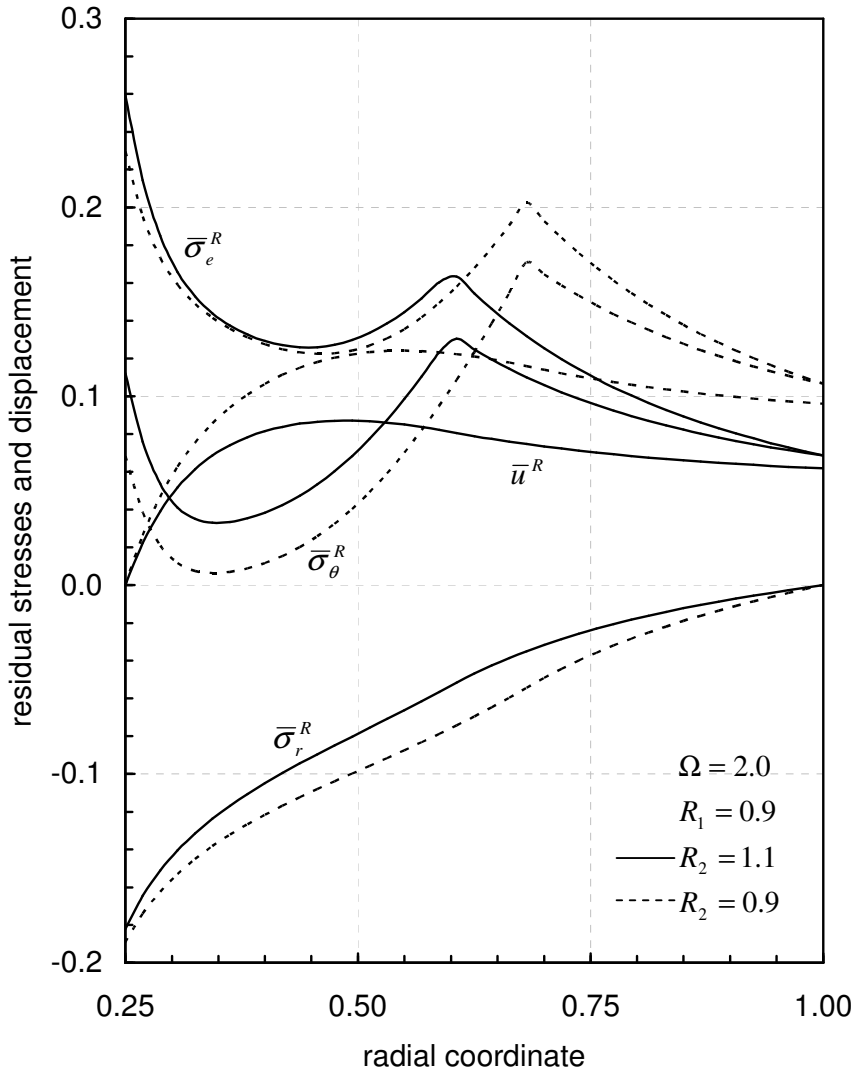

Figure 4.32 Effect of plastic orthotropy parameter R_2 on residual stress distributions for rotating disk with rigid inclusion.

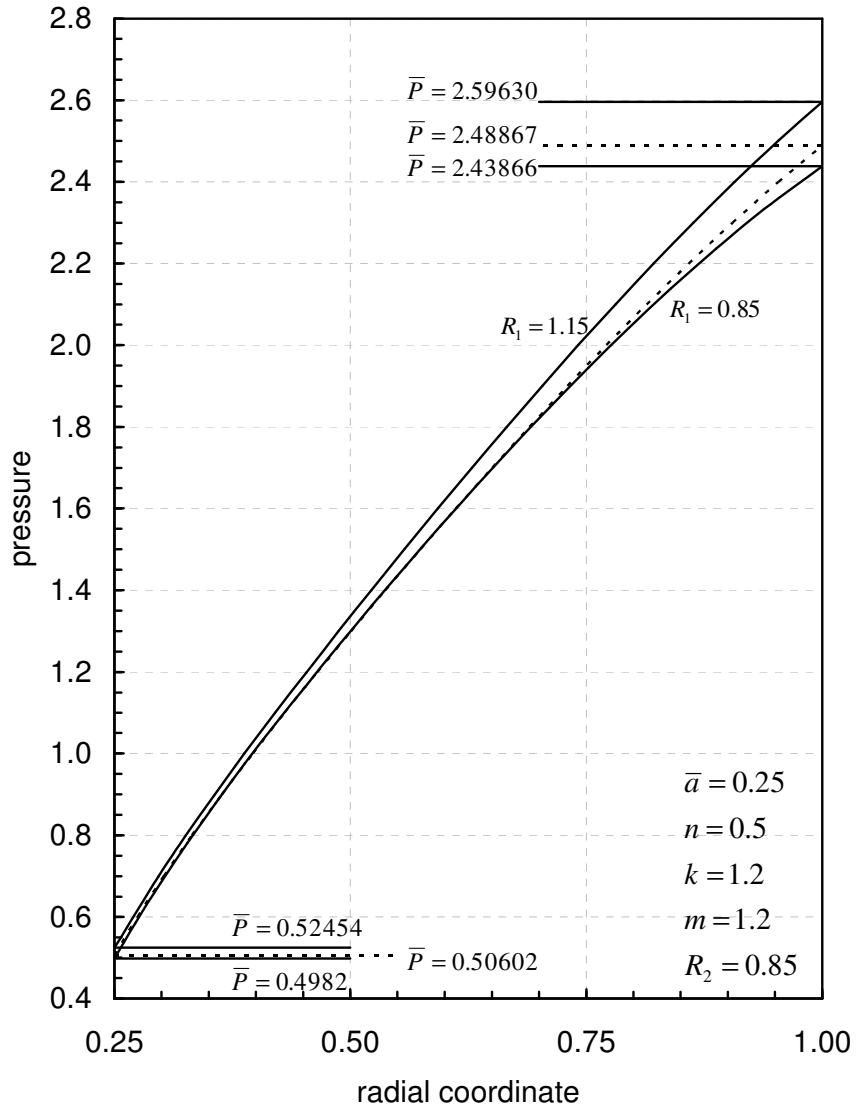

Figure 4.33 Propagation of elastic-plastic border radius with increasing angular speed due to effect of elastic orthotropy parameter R_1 for stationary annular disk subjected to internal pressure.

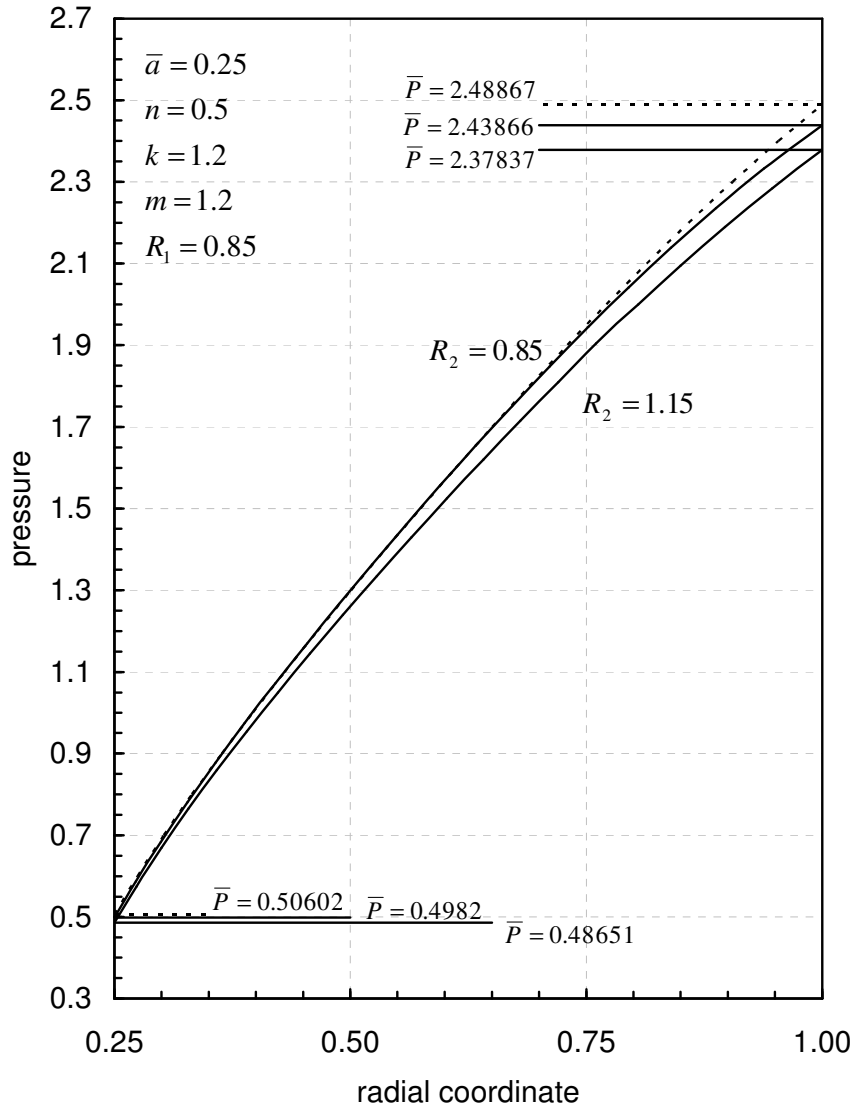

Figure 4.34 Propagation of elastic-plastic border radius with increasing angular speed due to effect of plastic orthotropy parameter R_2 for stationary annular disk subjected to internal pressure.

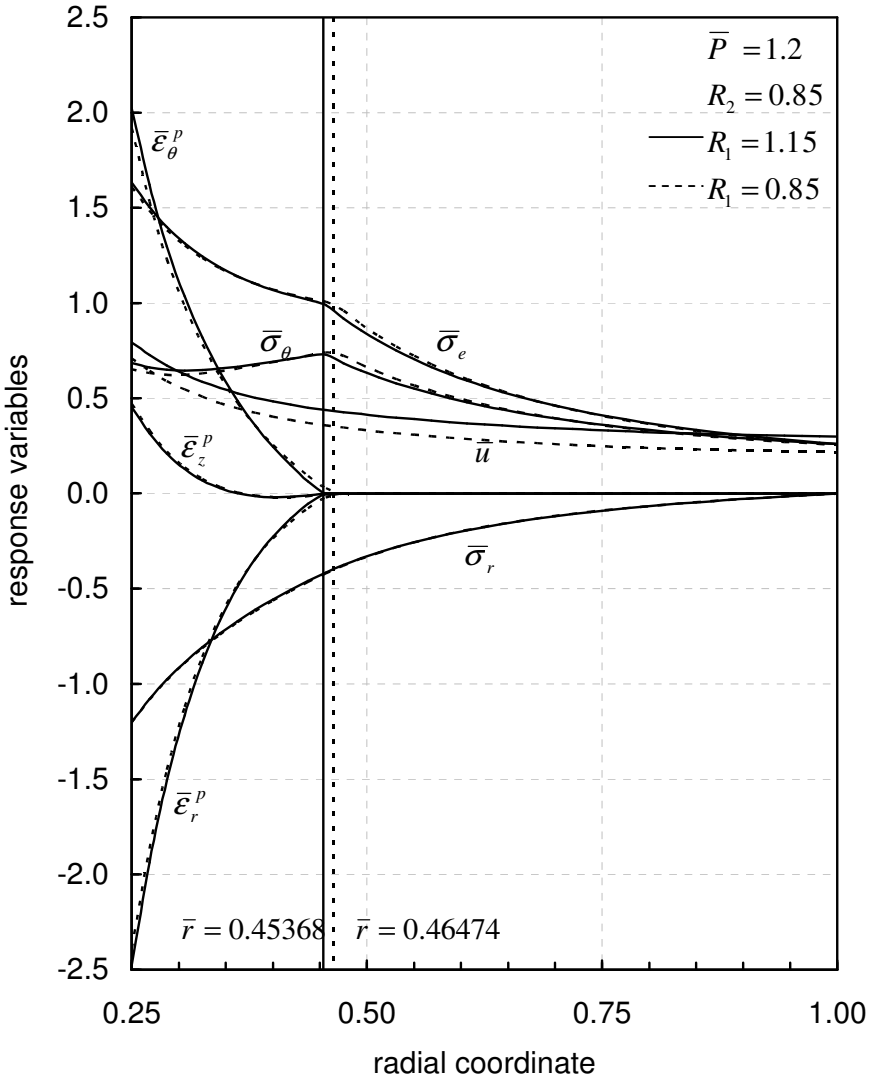

Figure 4.35 Effect of elastic orthotropy parameter R_1 on stress, strain and radial displacement distributions for stationary annular disk subjected to internal pressure.

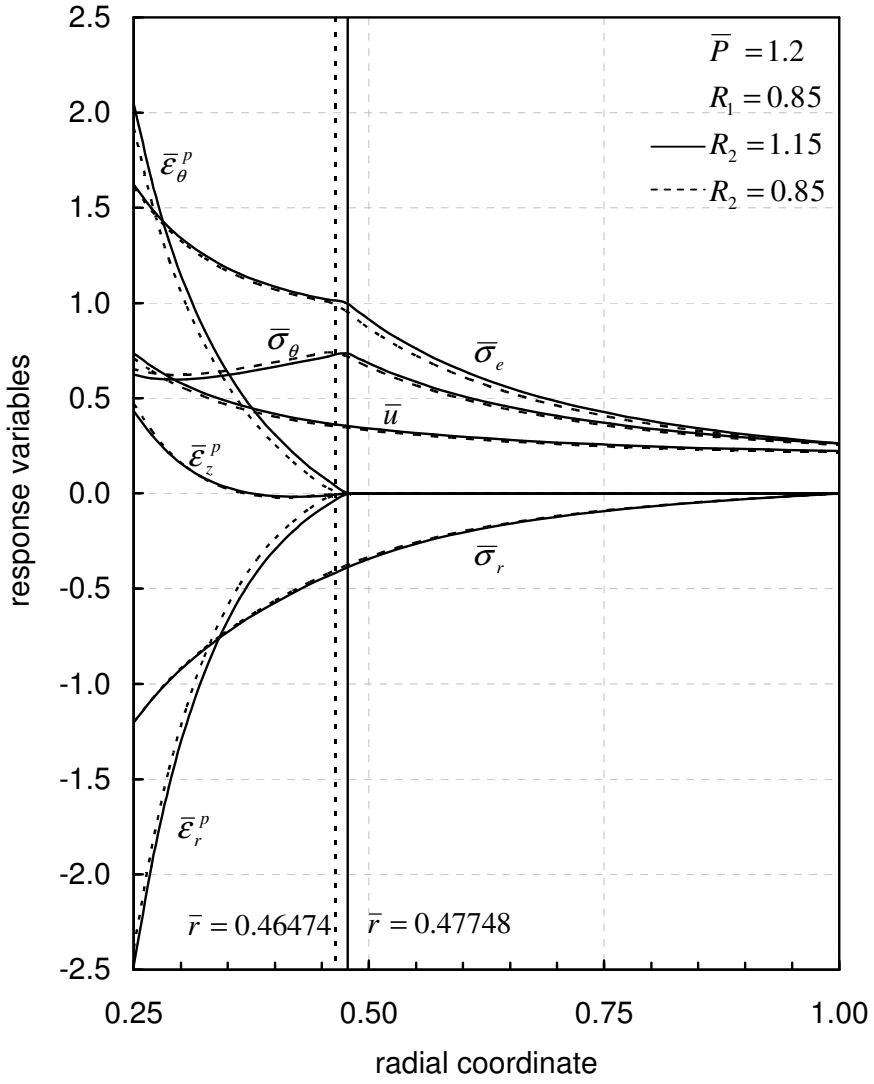

Figure 4.36 Effect of plastic orthotropy parameter R_2 on stress, strain and radial displacement distributions for stationary annular disk subjected to internal pressure.

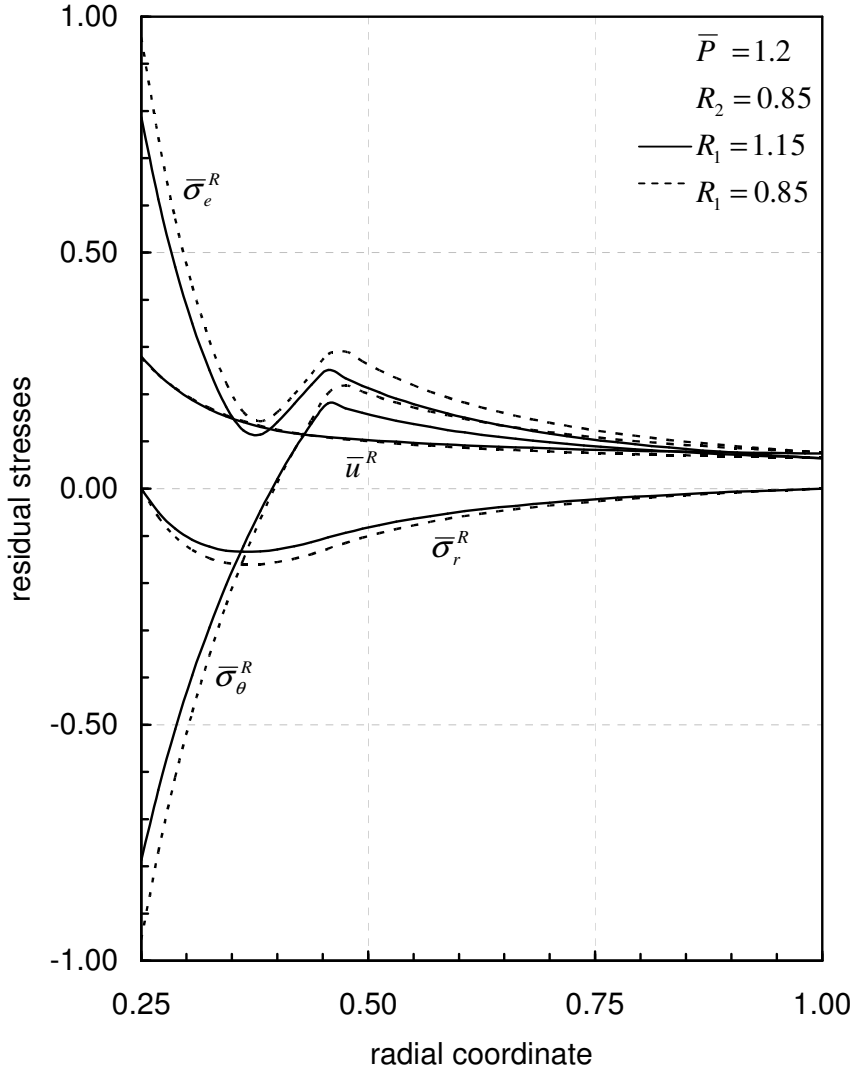

Figure 4.37 Effect of elastic orthotropy parameter R_1 on residual stress distributions for stationary annular disk subjected to internal pressure.

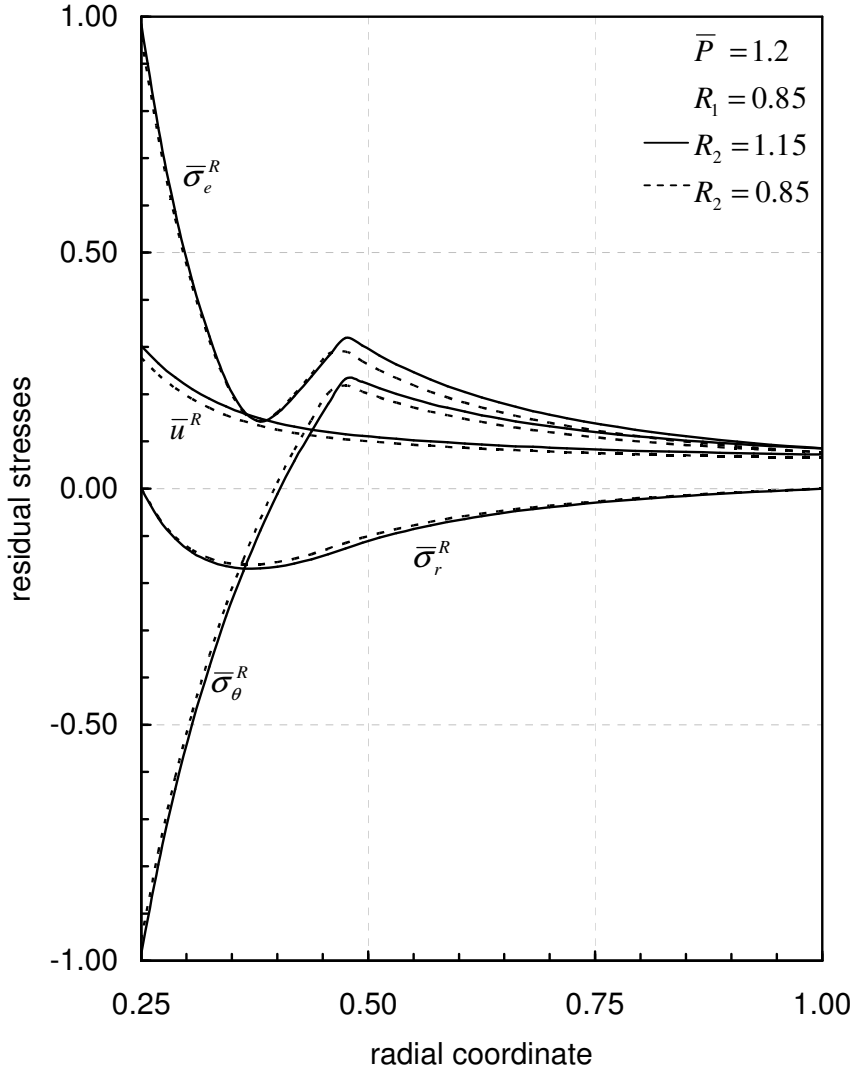

Figure 4.38 Effect of plastic orthotropy parameter R_2 on residual stress distributions for stationary annular disk subjected to internal pressure.

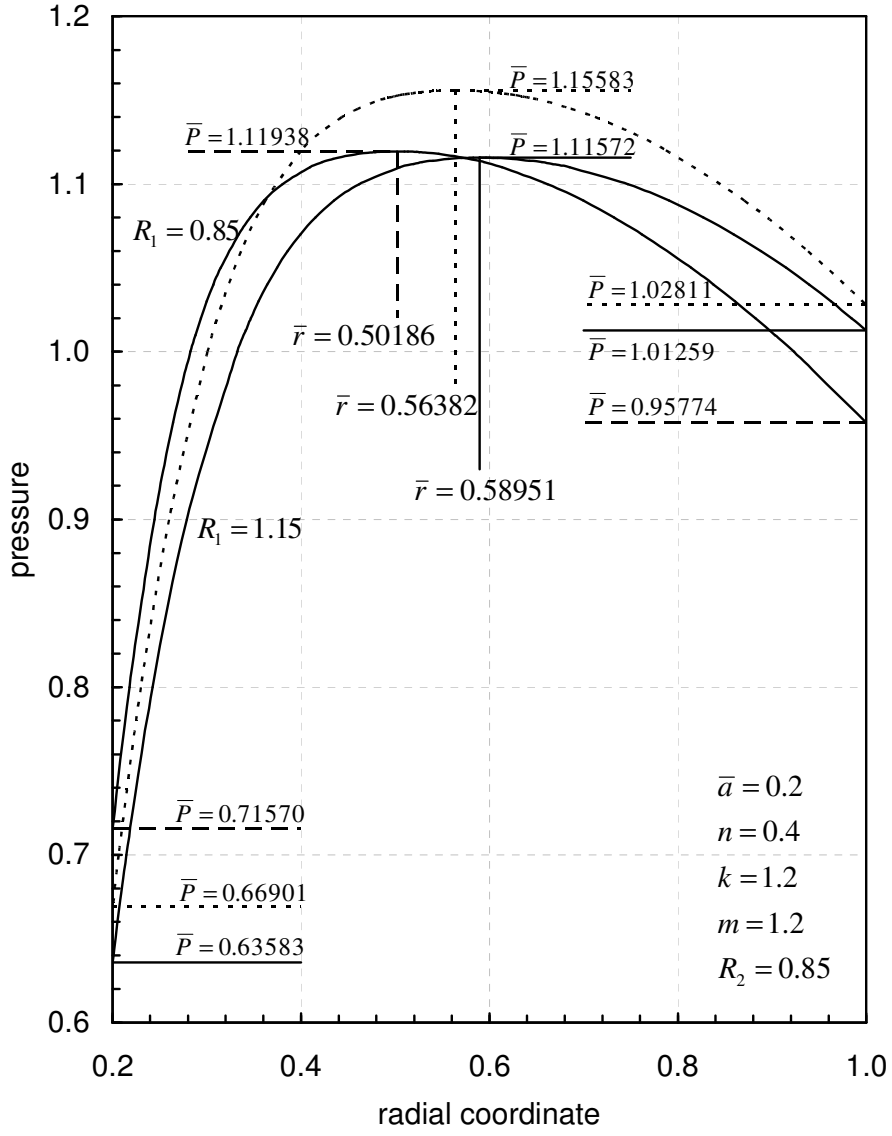

Figure 4.39 Propagation of elastic-plastic border radius with increasing angular speed due to effect of elastic orthotropy parameter R_1 for stationary annular disk subjected to external pressure.

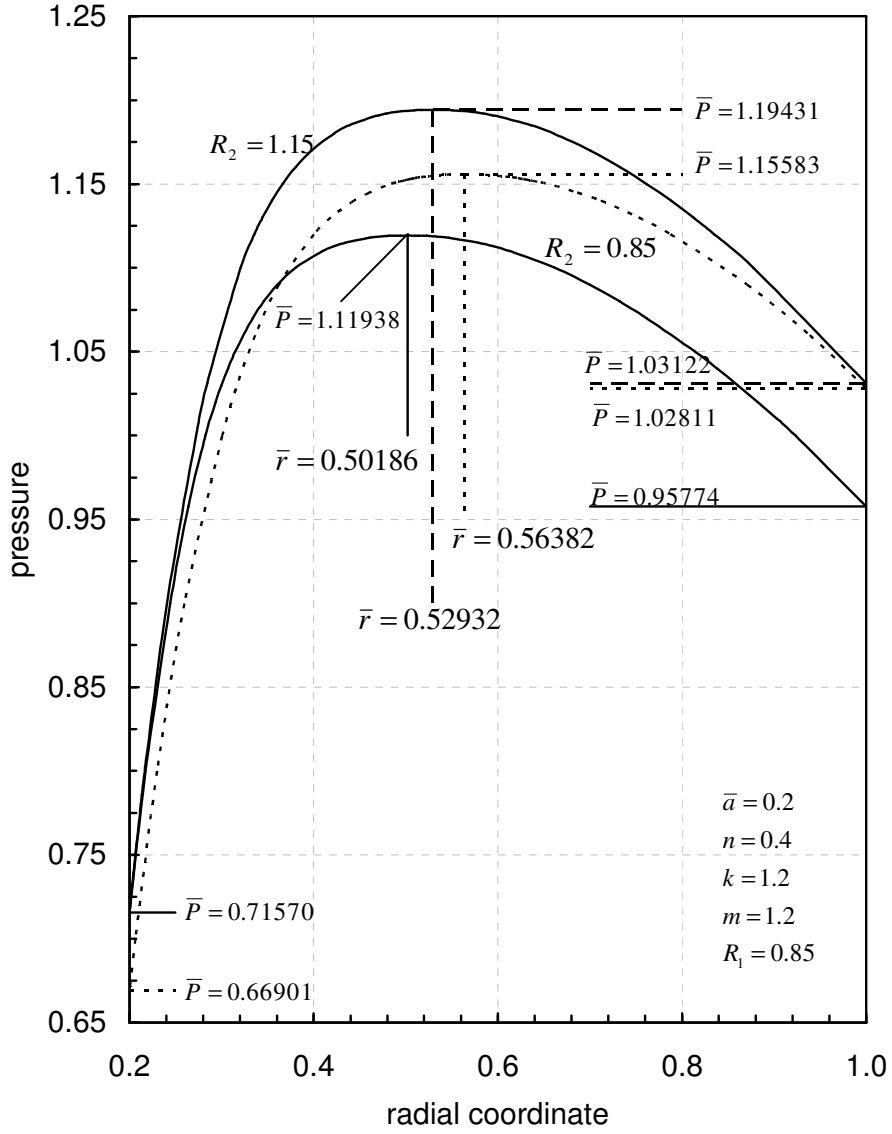

Figure 4.40 Propagation of elastic-plastic border radius with increasing angular speed due to effect of plastic orthotropy parameter R_2 for stationary annular disk subjected to external pressure.

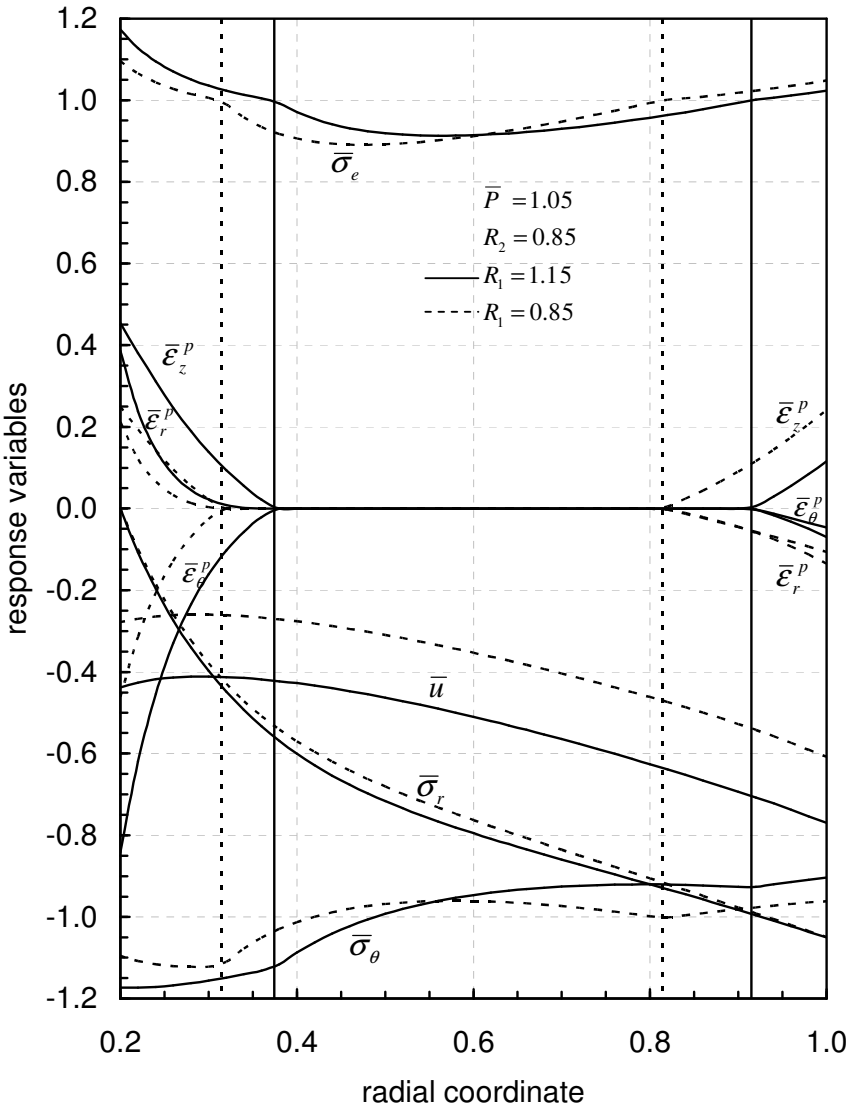

Figure 4.41 Effect of elastic orthotropy parameter R_1 on stress, strain and radial displacement distributions for stationary annular disk subjected to external pressure.

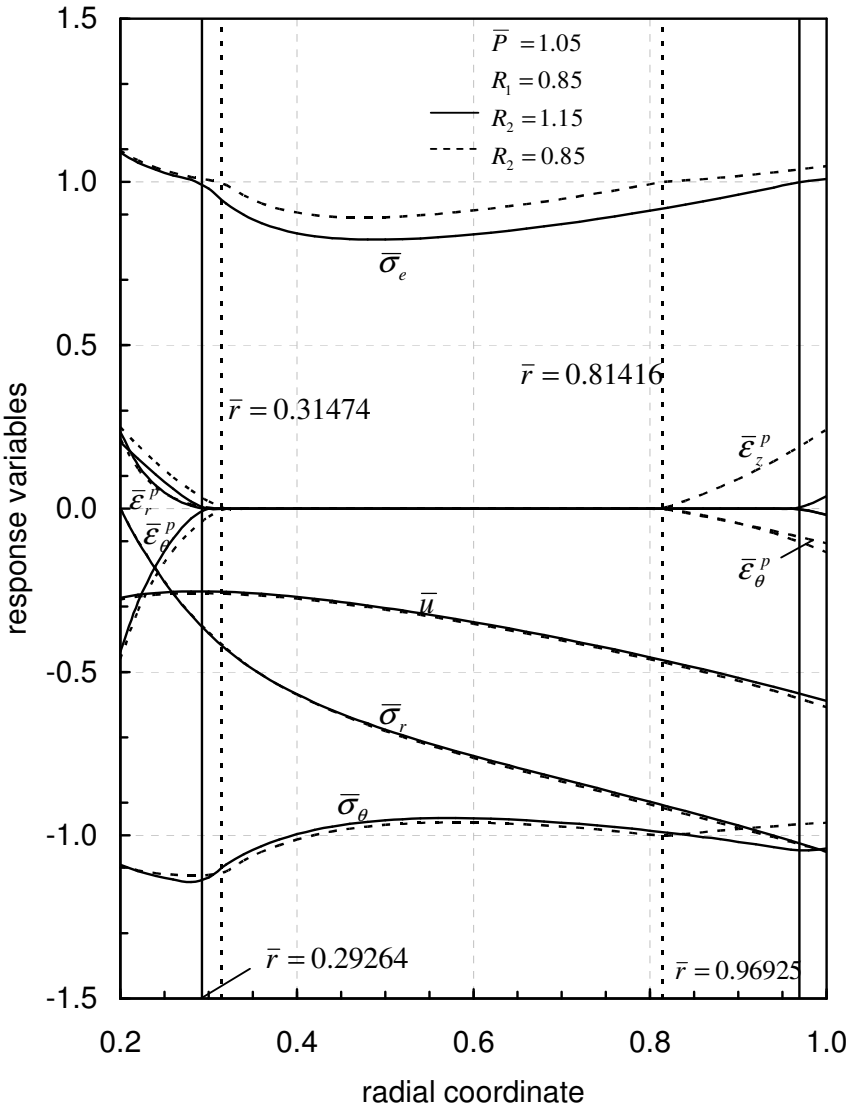

Figure 4.42 Effect of plastic orthotropy parameter R_2 on stress, strain and radial displacement distributions for stationary annular disk subjected to external pressure.

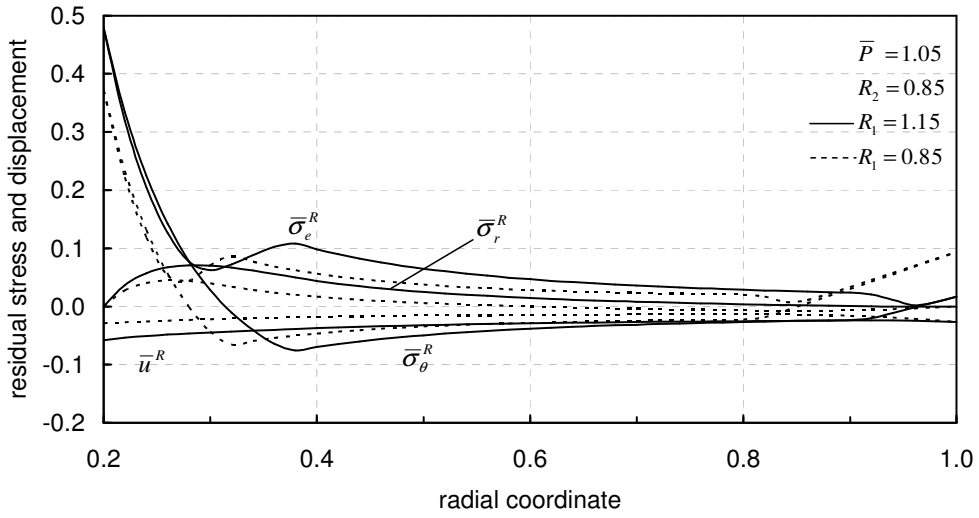

Figure 4.43 Effect of elastic orthotropy parameter R_1 on residual stress distributions for annular disk subjected to external pressure.

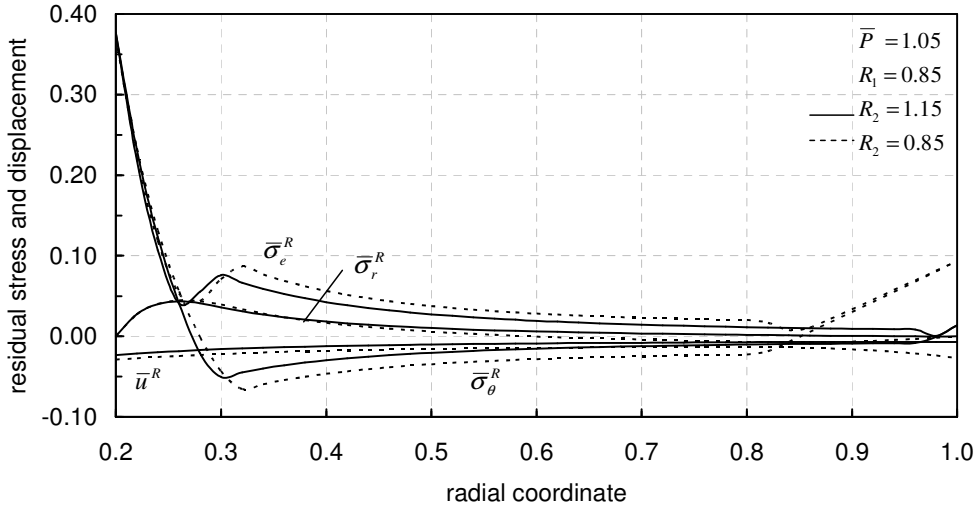

Figure 4.44 Effect of plastic orthotropy parameter R_2 on residual stress distributions for annular disk subjected to external pressure.

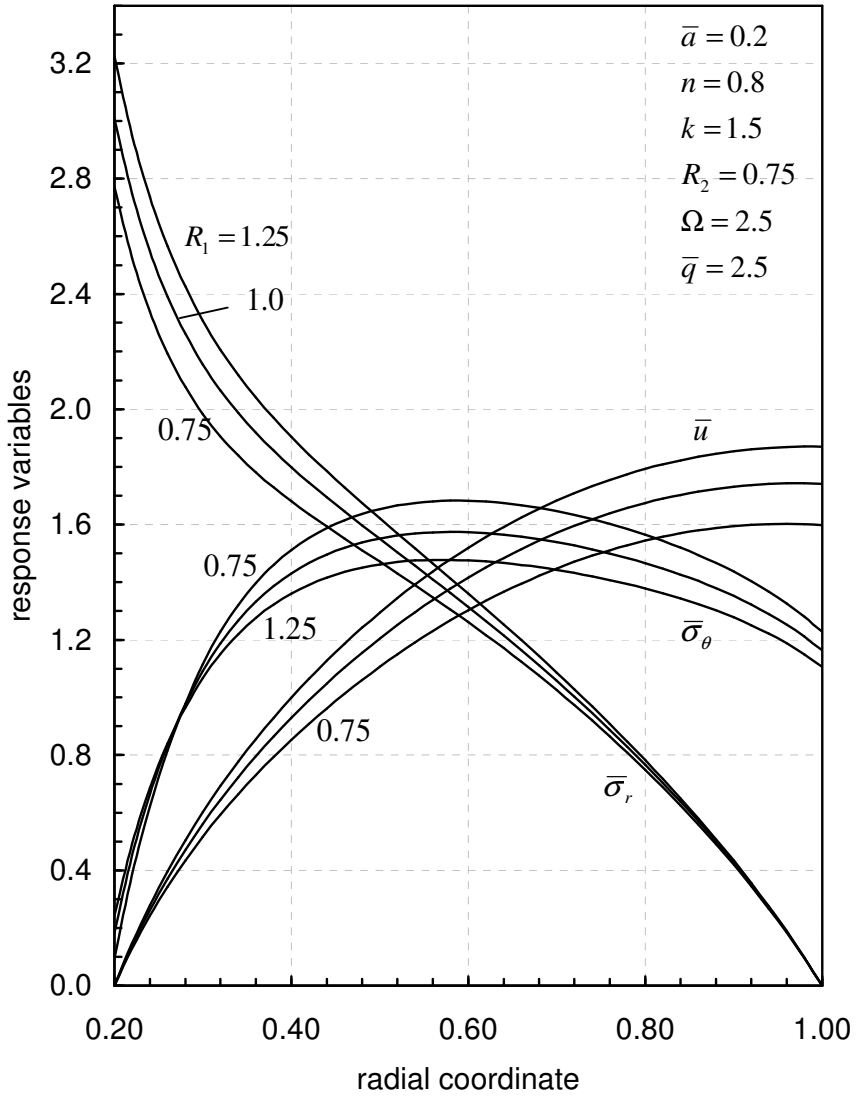

Figure 4.45 Effect of plastic orthotropy parameter R_1 on stress and displacement distributions for nonisothermal rotating disk with rigid inclusion.

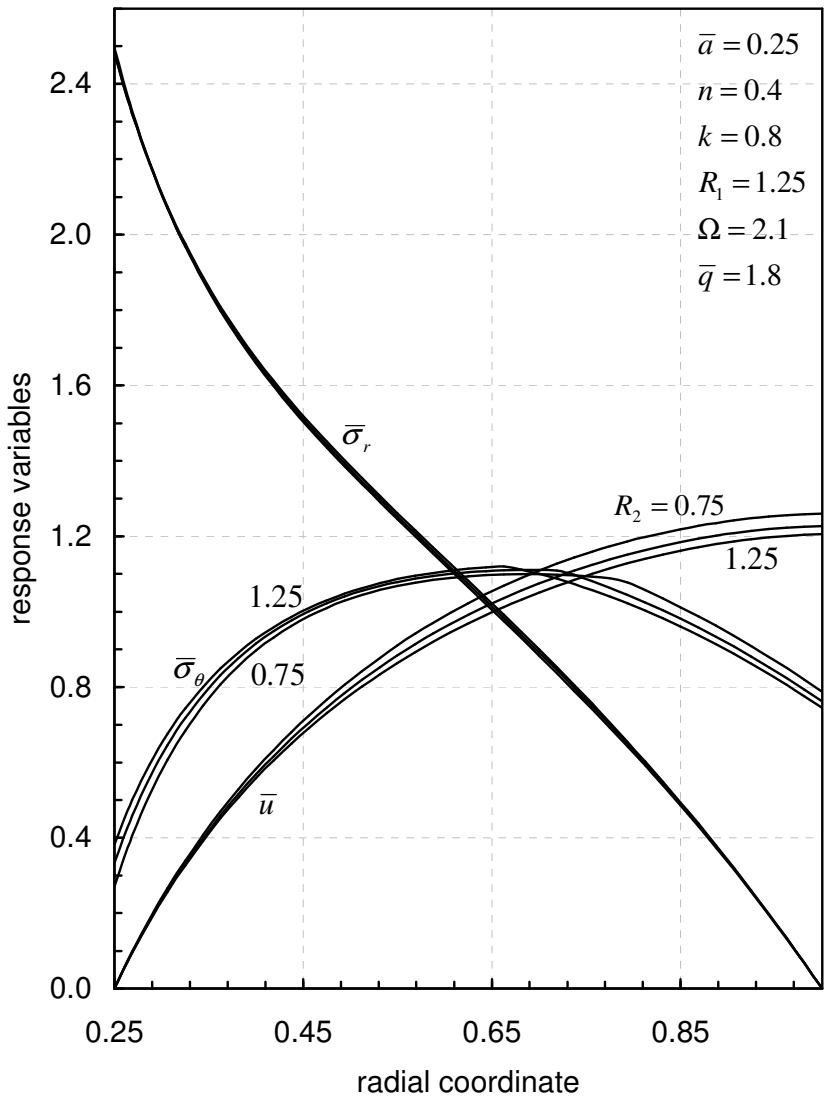

Figure 4.46 Effect of plastic orthotropy parameter R_2 on stress and displacement distributions for nonisothermal rotating disk with rigid inclusion.

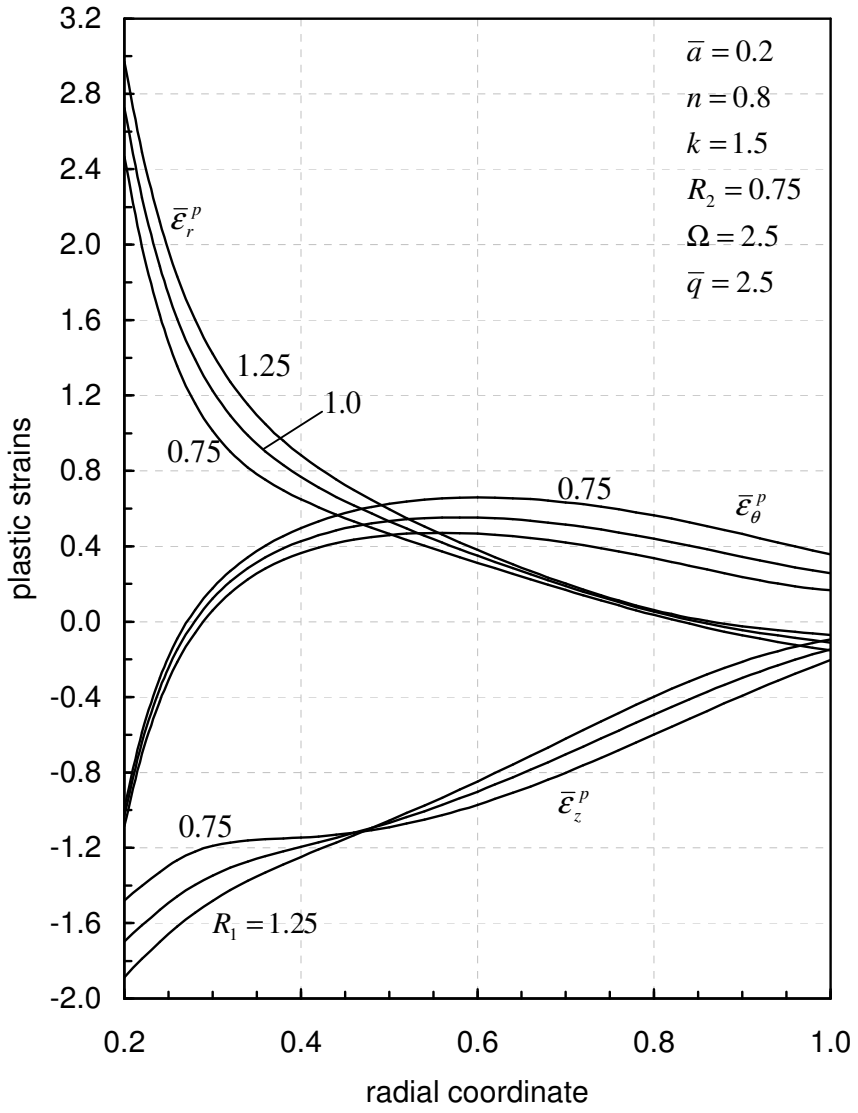

Figure 4.47 Effect of plastic orthotropy parameter R_1 on strains for nonisothermal rotating disk with rigid inclusion.

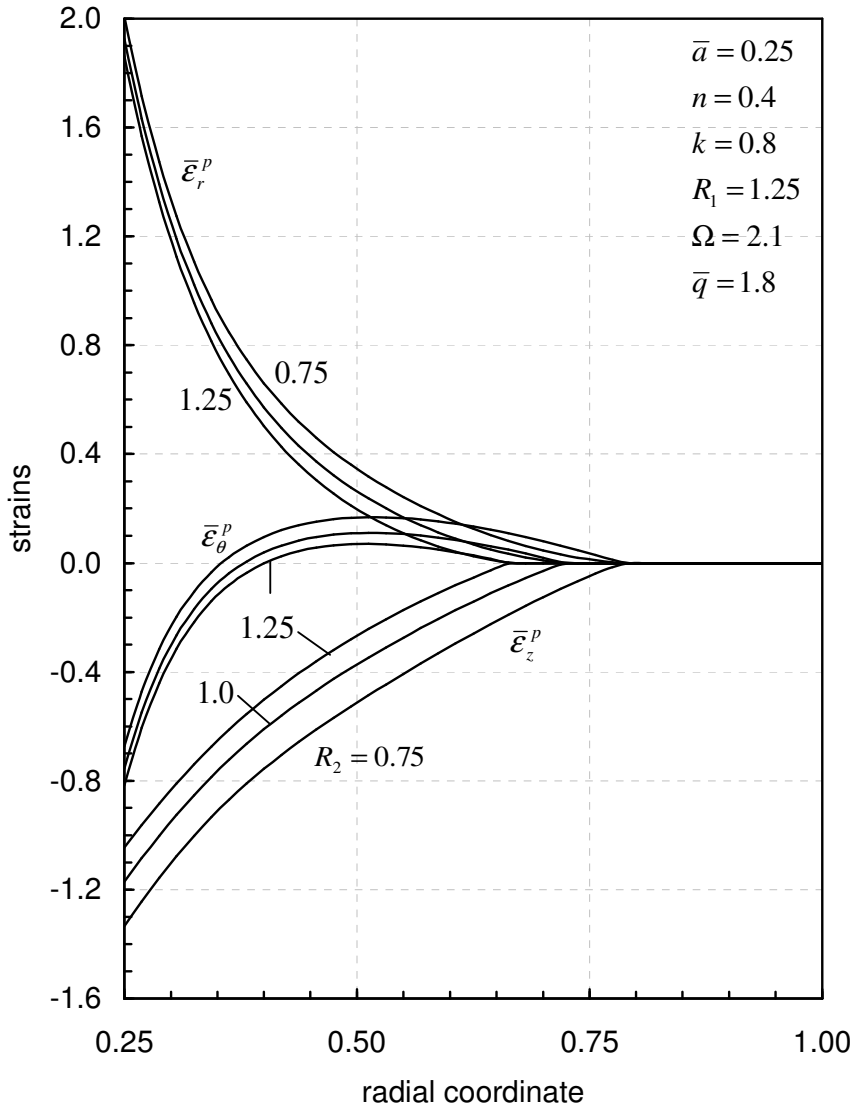

Figure 4.48 Effect of plastic orthotropy parameter R_2 on strains for nonisothermal rotating disk with rigid inclusion.

CHAPTER 5

CONCLUSION

In this study, an elastic-plastic rotating disk problem is investigated under various boundary conditions considering the orthotropy properties of material. In the five different cases, elastic and plastic orthotropy effects are taken into account. When the elastic and plastic orthotropy parameters R_1 and R_2, respectively, are equal to 1, the solution gives nonlinear strain hardening rotating isotropic disk with variable thickness. In general, it is seen that the plastic strains are affected strongly from plastic orthotropy and in the rotating disks working at high angular speed the size of plastic region decreases with increasing the degree of orthotropy. One of the important results of this research is that the effect of elastic orthotropic properties of the material on the residual stresses can be significant. Comparison between different cases considered here shows that the effect of plastic orthotropy is more significant under the rigid inner boundary condition.

REFERENCES

1. Timoshenko S.P., Goodier J.N., Theory of Elasticity, 3rd Ed.,McGraw-Hill, New York, 1970

2. Rees D.W.A., The Mechanics of Solids and Structures, McGraw-Hill, New York, 1990

3. Güven U.,Elastic-plastic stress distribution in a rotating hyperbolic disk with rigid inclusion. International Journal of Mechanical Sciences 40, 97-109, 1998.

4. Güven U., Elastic-plastic stresses in a rotating annular disk of variable thickness and variable density, International Journal of Mechanical Sciences 34, 133-138, 1992.

5. Güven U., Altay O., Elastic-plastic rotating solid disk with rigid casing, ZAMM 77, 867-870, 1997.

6. Güven U., The fully plastic rotating solid disk of variable thickness, ZAMM 74, 61-65, 1994.

7. Eraslan A.N., Von Mises yield criterion and nonlinearly hardening variable thickness rotating annular disks with rigid inclusion, Mechanics Research Communications 29, 339-350, 2002.

8. Eraslan A.N., Orcan Y., On the rotating elastic-plastic solid disks of variable thickness having concave profiles. International Journal of Mechanical Sciences 44, 1445-1466, 2002.

9. Eraslan A.N., Argeso H., Limit angular velocities of variable thickness rotating disks, International Journal of Solids and Structures 39, 3109-3130, 2002.

10. Eraslan A.N., Tresca's yield criterion and linearly hardening rotating solid disks having hyperbolic profiles, Forschung Im Ingenieurwesen/Engineering Research 69, 17-28, 2004.

11. Eraslan A.N., Stress distributions in elastic-plastic rotating disks with elliptical thickness profiles using Tresca and von Mises criteria, Zamm-Zeitschrift Fur Angewandte Mathematik und Mechanik 85, 252-266, 2005.

12. Eraslan A.N., Elastoplastic deformations of rotating parabolic solid disks using Tresca's yield criterion, European Journal of Mechanics/A-Solids 22, 861-874, 2003.

13. Eraslan A.N., Elastic-plastic deformations of rotating variable thickness annular disks with free, pressurized and radially constrained boundary conditions, International Journal of Mechanical Sciences 45, 643-667, 2003.

14. Eraslan A.N., Orcan Y., Elastic-plastic deformation of a rotating solid disk of exponentially varying thickness, Mechanics of Materials 34, 423-432, 2002.

15. Orcan Y., Eraslan A.N., Elastic-plastic stresses in linearly hardening rotating solid disks of variable thickness, Mechanics Research Communications 29, 269-281, 2002.

16. You L.H., Tang Y.Y., Zhang J.J., Numerical analysis of elastic-plastic rotating disks with arbitrary variable thickness and density, International Journal of Solids and Structures 37, 7809-7820, 2000.

17. You L.H., Zhang J.J., Elastic-plastic stresses in a rotating solid disk, International Journal of Mechanical Sciences 41, 269-282, 1999.

18. Rees D.W.A., Elastic-plastic stresses in rotating discs by von Mises and Tresca, ZAMM 79, 281-288, 1999.

19. Ma Guowei, Hao Hong, Miyamoto Yutaka, Limit angular velocity of rotating disk with unified yield criterion, International Journal of Mechanical Sciences 43 1137-1153, 2001.

20. Alexandrova N., Alexandrov S., Elastic-plastic stress distribution in a rotating annular disk, Mechanics Based Design of Structures and Machines 32, 1-15, 2004.

21. Alexandrova N., Alexandrov S., P. M.M Vila Real, Displacement field and strain distribution in a rotating annular disk, Mechanics Based Design of Structures and Machines 32, 441-457, 2004.

22. Durban D., Birman, V., Elastoplastic analysis of an anisotropic rotating disc, Acta mechanica 49, 1-10, 1983

23. Tütüncü N., Effect of anisotropy on inertio-elastic instability of rotating disks, International Journal of Solids and Structures 37, 7609-7616, 2000.

24. Çallıoğlu H., Topçu M., Tarakçılar A.R., Elastic-plastic analysis of an orthotropic rotating disc, International Journal of Mechanical Sciences 48, 985-990, 2006.

25. Alexandrova N., Alexandrov S., Elastic-plastic stress distribution in a plastically anisotropic rotating disk, J.Appl.Mech. (ASME) 71, 427-429, 2004.

26. Alexandrova N., Paulo M.M. Vila Real, Singularities in a solution to a rotating orthotropic disk with temperature gradient, Meccanica 41, 197-205, 2006.

27. Jain R., Ramachandra K., Simha K.R.Y., Singularity in rotating orthotropic discs and shells 37, 2035-2058, 1998.

28. Jain R., Ramachandra K., Simha K.R.Y., Rotating anisotropic disc of uniform strength, International Journal of Mechanical Sciences 41,639-648, 1999.

30. Johnson W., Mellor P.B., Plasticity for Mechanical Engineers, D. van Nostrand Company Ltd, 1970.

31. Hill R., The Mathematical Theory of Plasticity, Clarendon Press, Oxford, 1950.

32. Eraslan A.N.,Kartal M.E.,Stress distributions in cooling fins of variable thickness with and without rotation, Journal of Thermal Stress 28, 861-883, 2005.